

---

[Theses and Dissertations](#)

---

Spring 2016

# Developing and implementing a computer vision based surgical simulator for hip wire navigation

Steven A. Long  
*University of Iowa*

Copyright © 2016 Steven A. Long

This thesis is available at Iowa Research Online: <http://ir.uiowa.edu/etd/5555>

---

**Recommended Citation**

Long, Steven A.. "Developing and implementing a computer vision based surgical simulator for hip wire navigation." MS (Master of Science) thesis, University of Iowa, 2016.  
<http://ir.uiowa.edu/etd/5555>.



## DEVELOPING AND IMPLEMENTING A COMPUTER VISION BASED SURGICAL SIMULATOR FOR HIP WIRE NAVIGATION

by

Steven A. Long

A thesis submitted in partial fulfillment  
of the requirements for the Master of Science  
degree in Biomedical Engineering in the  
Graduate College of  
The University of Iowa

May 2016

Thesis Supervisors: Associate Professor Donald D. Anderson  
Professor Geb W. Thomas

Copyright by

Steven A. Long

2016

All Rights Reserved

Graduate College  
The University of Iowa  
Iowa City, Iowa

**CERTIFICATE OF APPROVAL**

---

**MASTER'S THESIS**

---

This is to certify that the Master's thesis of

Steven A. Long

has been approved by the Examining Committee for  
the thesis requirement for the Master of Science degree  
in Biomedical Engineering at the May 2016 graduation.

Thesis Committee:

---

Donald D. Anderson, Thesis Supervisor

---

Geb W. Thomas, Thesis Supervisor

---

Matthew D. Karam

---

Nicole M. Grosland

---

Joseph M. Reinhardt

## **ACKNOWLEDGEMENTS**

I would first like to start out by thanking my advisors, Don Anderson and Geb Thomas. They have both been phenomenal in providing guidance and direction on this project, as well as being patient with things when there were bumps along the path to success. I have thoroughly enjoyed working with both of them and look forward to our future endeavors.

I would also like to thank the members of the Orthopaedic Biomechanics lab for supporting this project with words of encouragement, honest feedback, and being my tireless guinea pigs for testing things out. A special thank you is deserved for Leah Taylor and Colleen Rink who helped immensely with this project. Truly, without the efforts of these two individuals much of this work would not have happened. Additionally Drew Kern was a great friend to talk to and bounce ideas off of throughout this project.

Lastly, I would like to acknowledge my strongest support system, my family and loved ones. There is no end to the many ways that you have helped me along this journey and for that I am forever grateful.

## **ABSTRACT**

Orthopaedic residency training is in the midst of a paradigm shift. Recent mandates from the Residency Review Committee (RRC) for Orthopaedic Surgery and the American Board of Orthopaedic Surgery (ABOS) are requiring that programs must provide structured motor skills training to first year residents. Although other surgical fields such as laparoscopic surgery have been using simulation tools to train incoming residents for over a decade, the orthopaedic field has lagged behind in developing these training tools. Given the need for orthopaedic training devices and the lack of currently available solutions to residency programs, this work has focused on developing a surgical simulator for the task of hip guide wire navigation. Hip wire navigation was targeted for this work because it is a core competency skill for surgical residents and few options currently exist for training residents on this task.

Much of this work focuses on the development of the wire navigation simulator. The simulator has six main components; a single camera interfaced with a Raspberry Pi (a credit-card sized computer), a series of three mirrors, a surrogate femur, a guide wire driver, a laser etched guide wire, and a laptop. These components interact to create virtual radiograph images that the resident can use to place the guide wire inside the bone. The goal in developing this simulator is to provide a platform which enables residents to acquire the skill of hip wire navigation in a safe environment and eventually transfer that skill into the operating room.

Assessment of the simulator has shown that the guide wire can be located in bone within 1.5mm of its true position and less than a degree of its true trajectory. This level of accuracy is sufficient for providing residents with a training tool to practice their technique on.

In training with resident surgeons, initial trends show that practicing with the simulator can result in an improvement in one's technique. Residents who have trained with the simulator

show a decrease in both the amount of radiographic images required to complete the procedure and the amount of time required to perform the procedure in a pseudo operating room environment. While more work is needed to be done to show the significance of this trend, this work has achieved its goal of providing residents with a safe platform for practicing the task of hip guide wire navigation.

## **PUBLIC ABSTRACT**

Orthopaedic residency training has remained largely unchanged for the past century. The common form of training over this time period has been an apprenticeship model where residents observe experts performing a surgery and then attempt this surgery in the operating room (OR) under the supervision of an expert surgeon. This has been shown to put patients at a higher risk and extend the time spent in the operating room.

Recent mandates have required that resident surgeons have increased motor skills training outside of the operating room in their first year of residency. Motor skills training outside of the OR is intended to provide residents with the surgical skills they need before practicing on a patient. This work has focused on developing a surgical simulator for the task of hip wire navigation, a complex motor skills task that would benefit greatly from practice outside of the OR. After developing the surgical simulator, this work also shows how the tool can be implemented at residency programs to help train resident on this task.

## TABLE OF CONTENTS

LIST OF TABLES.....	viii
LIST OF FIGURES .....	ix
Chapter 1: Literature Review.....	1
A Brief History of Surgical Education: .....	1
A Need for Surgical Simulation:.....	3
Brief History of Simulation: .....	6
Deliberate Practice: .....	9
Simulation in Laparoscopic Surgery:.....	13
Simulation in Orthopaedics: .....	16
Simulation in Hip Fractures:.....	19
Summary:.....	24
Chapter 2: Simulator Design.....	25
Introduction:.....	25
Simulator Design Parameters:.....	25
Simulator Conceptual Overview:.....	28
Design Iteration 1:.....	33
Hardware Design: .....	33
Software Development: .....	37
Design Iteration 1 Issues:.....	46
Design Iteration 2:.....	47
Hardware Design: .....	47
Software Development: .....	51
Chapter 3: Simulator Assessment .....	58
Simulator Accuracy: .....	58
Accuracy Results: .....	61
Discussion:.....	63
Chapter 4: Simulator Implementation.....	64

Training with Residents: .....	64
Training Results: .....	68
Discussion:.....	73
Chapter 5: General Discussion and Future Work .....	75
Simulator Strengths and Limitations: .....	75
Future Work: .....	77
References .....	79
Appendix 1 .....	84

## **LIST OF TABLES**

Table 1 - Hardware Design Contributions .....	51
Table 2 - Wire Accuracy Results Across Multiple Locations .....	63

## LIST OF FIGURES

Figure 1 - The training mannequin developed by Madame du Coudray to train midwives. Image taken from [22]. .....	8
Figure 2 - An illustration of how expert performers are constantly learning and relearning their craft. Entering into the autonomous phase of learning can lead to what is described as “arrested development” [26]. .....	10
Figure 3 - A chart illustrating the difference between hours of practice by varying levels of skilled violin players. Graphic taken from [25]. .....	11
Figure 4 - An image of an early development of the MISTELS system. Image taken from [35].	14
Figure 5 - The FORS skill board containing six stations to assess different orthopaedic skills... .	17
Figure 6 - An image of a lag screw being placed inside the virtual bone in the Bonedoc DHS simulator. Image taken from [49]. .....	18
Figure 7 - Graphics depicting the three categories of intertrochanteric hip fractures. Image taken from [56]. .....	20
Figure 8 - Radiographic images showing an implanted dynamic hip screw. In some cases an additional screw is added superiorly to provide additional stability to the fracture. Image taken from [59]. .....	21
Figure 9 - This image describes the calculation of the TAD. It is a sum of the distances in both the anterior-posterior and lateral views. Image taken from [60]. .....	22
Figure 10 - A cross section of a proximal femur illustrating the changes in bone density depending on the location in bone. Image taken from [65]. .....	27
Figure 11 - A schematic diagram depicting the flow of data when using the simulator. ....	29
Figure 12 – A system of equations can be arranged to solve for the 11 L and 11 R image parameters. Image taken from [68]......	31
Figure 13 - A display of the first iteration of the wire navigation simulator. The laptop, guide wire, and guide wire driver are not shown in this image. ....	34
Figure 14 - The laser scan of the proximal femur mounted to the calibration object.....	35
Figure 15 - The wire address scheme is shown here. Addresses are separated by a 2.5mm thick line.....	36

Figure 16 - The results of the edge detection on the left image are shown here. It is noticeable that one side of the wire has a clean edge to it while the other side has missing gaps that were missed in the edge detection.....	38
Figure 17 - The results of the Hough transform line detection on the left image show the wire edges outlined in green.....	40
Figure 18 - The results of the horizontal edge detection. The original image of the wire is shown on the left with the resulting edge image on the right.....	41
Figure 19 - On the left, the stretched horizontal edge image can be seen with lines labeled resulting from the Hough transform. On the right these lines can be seen mapped back on to the original image.....	42
Figure 20 - This system of equations allows the X, Y, and Z coordinates of the wire vector to be back projected [68]. The system is again solved using a Moore-Penrose pseudo-inverse method.....	43
Figure 21 - An example of a virtual AP radiograph that could be presented to a resident.....	45
Figure 22 - On the left is a rendering of the simulator in Creo. On the right is an image of the physical simulator. The LED lights are not visible in either image.....	47
Figure 23 - The calibration object and proximal femur can be seen registered in Geomagic. Additional calibration points on the top surface of the calibration object are not visible from this view.....	49
Figure 24 - The new wire etched pattern is shown here.....	50
Figure 25 - The outline of the wire is found in the left image of the new simulator.....	53
Figure 26 - On the left is the cropped region of wire before adaptive histogram equalization is applied. On the right is the cropped wire after adaptive histogram equalization is applied.....	54
Figure 27 - The resulting binary images from the templating matching algorithm.....	55
Figure 28 - The start and stop of each etched black line can be seen here for the left image. Similar results are produced in the right image.....	56
Figure 29 - The target sawbones are pictured here. The target slots are shown to cover the workspace provided in the window of the soft tissue envelope.....	59
Figure 30 - One of the laser scans of the copper slotted sawbones can be seen here. The wires have all been aligned and projected into the coordinate space of the sawbones femur.....	60

Figure 31 - The wire error based on guide wire position is shown here. Wires colored in green have less than 1mm of error on average. Yellow wires have errors ranging between 1 and 2mm. Blue wires have errors ranging between 2 and 3mm. Red wires have an average error greater than 3mm. ....	62
Figure 32 - The schedule used to train the resident is shown here. ....	65
Figure 33 - The level 1 interface is shown here. On the right, an AP radiograph is shown. The green path in the virtual image provides a target path for the resident when placing the guide wire. Simulator tips and quantitative metrics of performance are displayed on the left half of the screen. ....	67
Figure 34 - The average simulator score across four trials is shown here. A negative trend in score, or improvement, is clearly visible in this chart. ....	68
Figure 35 - The average procedure time across four trials is shown here. ....	69
Figure 36 - The average number of fluoro images used across four trials is shown here. ....	69
Figure 37 - The average tip apex distance across four trials is shown here.....	70
Figure 38 - Group 1 and Group 2 C-arm exercise scores are shown here. The black line indicates that practicing with the simulator occurred between the trial numbers. ....	71
Figure 39 - Group 1 and Group 2 C-arm procedure duration over three sessions is shown here. 71	
Figure 40 - The number of radiographic images used for Group 1 and Group 2 in the C-arm exercise is shown here. ....	72
Figure 41 - The TAD results for Group 1 and Group 2 from the C-arm procedure is shown here. ....	72
Figure 42 - Group 1 and Group 2 results are combined into pre and post practice on the simulator. A trend of improving scores can be seen in this data. ....	73
Figure 43 - Examples of different address markings are shown here. Not all combinations for $k=2$ are shown here. ....	85
Figure 44 - The overall etch pattern on the wire is shown here. The pattern begins on the left and moves to the right.....	85

## **Chapter 1: Literature Review**

### A Brief History of Surgical Education:

Surgical training in the United States has seen many changes evolve over the last three centuries. Prior to the establishment of the United States, most surgeons had little formal education, if any. The first hospital to be constructed in the colonies was the Pennsylvania Hospital, opening in 1751 [1]. Like most systems around the world at the time, the Pennsylvania Hospital adopted the apprenticeship model for training new surgeons. In this model, attending physicians at the hospital had students follow them around and help where needed. Although this was an unstructured and unregulated form of education, most apprenticeships endured for 5 years. At the end of this apprenticeship, students were released and given a certificate proving their training [1]. Also of importance to note is that the hospital had the first surgical amphitheater, often used for anatomical dissections and observing surgical procedures [2]. It wasn't until 1765 that the first medical school opened, the Medical College of Philadelphia. Surprisingly for the times, the medical school had rather strict admissions requirements. Applicants were required to have "(1) apprenticeship for 3 years to a reputable physician, (2) education in liberal arts, mathematics, and natural history, (3) knowledge of Latin and, preferably, French as well" [3]. The curriculum involved two seven month sessions and covered instruction on "the nature and treatment of chronic diseases, ulcers, wounds, fractures, and all the operations of surgery" [4].

Medical schools began to slowly propagate through the major cities of the United States, such as Boston, Philadelphia, and New York. However, as the population grew rapidly from seven to seventeen million between 1810 and 1840, the need for surgeons grew and the standards

for training them fell. In this era, no educational prerequisites were required and anyone that could pay their tuition for the two year program was given a doctorate [4].

For the majority of the 19<sup>th</sup> century, little improvement was made in the field of surgical education. That said, several attempts at improving surgical education were made. For instance, schools such as the University of Michigan Medical School and the Chicago Medical College added a graded curriculum and the use of scientific laboratories. Additionally, in 1869, the American physician Charles W. Elliot suggested adding written examinations in order to complete a degree of Doctor of Medicine. However, a professor of surgery at Harvard, Henry Jacob Bigelow, replied “the students should not be expected to pass written examinations since half of them could hardly write” [5]. With so few standards in the field of surgical training, it is understandable that when the Royal College of Surgeons was founded in 1800, one member noted “there is no more science in surgery than in butchering” [6].

Near the turn of the 19<sup>th</sup> century and at the beginning of the 20<sup>th</sup> century, two main voices created landmark shifts in the education of surgeons; those of Dr. William Osler and Dr. William Halsted. Although the majority of the credit for our current system of training residents is often given to Dr. Halsted, Dr. Osler proposed a similar system in 1890, some fourteen years before Halsted’s landmark speech at Yale [7]. In the Osler system of training, a closer relationship between the student and instructor was emphasized. In this system, multiple surgical residents of varying surgical experience work with multiple faculty members. It is noted that “staff physicians are not merely occasional lecturers or distant figures, but are actively involved in instructing residents while seeing patients during clinics” [7]. Many of these themes can be seen in the system for training surgeons today.

Prior to his landmark speech in 1904, William Halsted studied in Germany for several years. Upon his return, his colleague Dr. Osler remarked that he was “very much *verdeutsched* [made German] and held that there were only three or four good surgeons in the world and all of them were German” [4]. Not surprisingly, much of Halsted’s ideas on training surgeons were taken from the German model at the time. In his speech at Yale Halsted remarked, “The hospital, the operating room and the wards should be laboratories, laboratories of the highest order, and we know from experience that where this conception prevails not only is the cause of higher education of medical science best served, but also the welfare of the patient is best promoted” [6]. In his model of training, Halsted proposed that residents should receive increasing responsibility with each advancing year. In this system, the average length of residency was 8 years, 6 years as an assistant and 2 years of service as the house surgeon [8]. Halsted’s model was a much more structured form of training than anyone had previously proposed or seen in the U.S. and led to a much better trained surgeon. This methodology began to slowly gain support in hospitals across the U.S., and in 1928 the American Medical Association approved the underlying principles for residencies and fellowships [9]. For the better part of the remaining 20<sup>th</sup> century, William Halsted’s model remained the best and most widely used form of surgical training. However, as technologies improve and cultures change, so too must the way we train our surgical residents.

#### A Need for Surgical Simulation:

When the laparoscopic cholecystectomy first entered the medical mainstream in the 1980’s it was touted as one of the greatest advancements in surgery since ether anesthesia [10]. This, along with other laparoscopic procedures offered the promise of having reduced operative trauma, reduced incidence of major wound complications, shorter hospital stays, and reduced duration of short-term disability [11]. For the most part, these promises are not empty, so long as

the surgeon performing the procedure is well trained. However, it has often been stated that with the increased popularity of these procedures, the expansion of the laparoscopic cholecystectomy was “the biggest unaudited free-for all in the history of surgery” [10]. In other words, many surgeons were performing this surgery after only a brief and inadequate amount of training. In a study done in New York in 1993, it was noted that the rate of the cholecystectomy had increased by 21% since the introduction of the laparoscopic cholecystectomy. More importantly though, the rate of serious injury may have been 15 times higher than that of an open cholecystectomy [12]. Clearly a majority of the surgeons performing these procedures needed additional practice in a safe environment before performing on a patient.

Apart from new technologies, a shifting culture can also create a need to change the way surgeons are trained. Since the creation of the Occupational Safety and Health Administration (OSHA) in 1970, there have been increased efforts to make sure that across all occupations, there are safe working conditions [13]. An incident in 1984, often referred to as the “Libby Zion affair”, exposed that perhaps the working conditions for surgeons and their residents are not as safe as they should be. In this event, a young woman died in the middle of the night while being operated on by an unsupervised and tired first-year resident [2]. Although some years later, in 2001 the Accreditation Council for Graduate Medical Education (ACGME) came out with a set of standards on the amount of time a resident could spend working each week. Although there are other provisions to these standards, the main takeaway was that residents could spend at most 80 hours each week in training [13]. Just two years later, the European counterpart to this came in the form of the European Working Time Directive (EWTD) which enforced “a limit to weekly working hours, which must not exceed 48 hours on average, including any overtime” [14]. With these strict limits on working hours, it is fair to say that the apprenticeship model is changing and

that residents may not be getting the same amount of exposure or practice they used to. This again presents the need for an area to practice one's skills and techniques in a directed manner that will promote technical competency.

In addition to reducing resident hours, surgeons are also expected to make fewer errors in today's society. In the study published by the Institute of Medicine in 1999, titled "To Err is Human: Building a Safer Health System", it was reported that up to 98,000 deaths occur each year due to medical error [15]. It goes on to further state that "more than two-thirds (70 percent) of the adverse events found in this study were thought to be preventable, with the most common types of preventable errors being technical errors (44 percent)" [15]. Although the report does clarify that many of the errors are systems errors and that surgeons and physicians are not solely at fault, clearly there is room for improvement in the technical abilities of surgeons still today. As a result, a main recommendation coming from this study was that patient safety programs be created that "establish interdisciplinary team training programs for providers that incorporate proven methods of team training, such as simulation" [15].

Seven years following this report, a study by Bell et al. examined whether or not surgeons were getting the proper exposure during residency programs to graduate as competent surgeons. In this study, an electronic survey was sent to 254 accredited general surgery programs in the US. The survey identified 300 procedures that were categorized by the following criteria; A – "graduating general surgery residents should be competent to perform the procedure independently", B – "graduating general surgery residents should be familiar with the procedure, but not necessarily competent to perform it", and C – "graduating residents neither need to be familiar with nor competent to perform the procedure" [16]. Of the 300 procedures identified, 121 were placed in category A, requiring competency by graduation. In the survey responses,

containing data on 1022 residents, only 18 procedures were performed on average more than 10 times during the residency. It was especially noted that “for 63 of the 121 procedures, the mode (most commonly reported) experience was 0” [16]. This article suggests that under the current paradigm, residents are not getting the exposure that directors expect them to be graduating with. Simply hoping that residents will experience this wide variety of procedures during their residency is a poorly structured system that is not meeting expectations.

As has been seen, with the development of new and challenging surgical techniques, a shifting culture of reduced work hours, and an expectation for greater patient safety and fewer errors, the apprenticeship model will no longer be sufficient in training the surgical residents of today. Rather, surgical residents need a safe environment where they can acquire their surgical skills quickly and without risk to the patient. This environment lies in the world of surgical simulation.

#### Brief History of Simulation:

Simulation is a tool that has been used in medical education for almost a millennium. Dating back to 1027 during the Song Dynasty in China, life sized statues were used for teaching the placement of acupuncture needles. Surprisingly advanced for the time, these simulators had 354 open holes on the body that could be pierced by acupuncture needles [17]. The statues were coated in wax and filled with a liquid so that when a needle was placed in the correct position, the liquid was released, thus providing crucial feedback to the trainee [18]. This first statue is often referred to as the “Bronze Statue of Acupuncture”, named for the materials it was constructed from [19].

Several hundred years later in France, the first patient specific simulator was used. In 1559 during a jousting tournament, a lance pierced the helmet of King Henry II of France. The Royal surgeon at the time did not think that the king would survive given the development of infection at the wound site, and determined that the remaining wood needed to be removed. Although barbaric and unethical, in an effort to practice the surgery, four criminals were beheaded and had broken spears thrust into their head at approximately the same location as the King [20]. Unfortunately, the surgery was unsuccessful and the king eventually passed away. Although this was certainly not an ethical form of simulation, it did provide a means for practicing the surgery before it was actually performed on the King.

A name that should get a great amount of credit for developing one of the earliest and most practical skills training simulators is Angelique Marguerite Le Boursier du Coudray. Madame du Coudray was commissioned by King Louis XV to teach midwife skills throughout France to reverse the trending population decline. Du Coudray then designed a life-sized mannequin representative of the female torso, genitalia, and upper thighs. It had a removable uterus and a drawstring that allowed for cervical dilation. It also included a life-sized newborn infant, a 7 month old fetus, and twins as seen in Figure 1. Sponges were added to release clear and red liquids at appropriate times during the birth [21]. Du Coudray was quoted as saying “we have the advantage of students practicing on the machine and performing all the deliveries imaginable. Therein lies the principal merit of the machine” [17]. Well ahead of her time, Madame Coudray also said, “the machines I leave with surgeons must be used each year to renew the lessons for the country women”, advocating for continual practice and renewal of skills [17].



Figure 1 - The training mannequin developed by Madame du Coudray to train midwives. Image taken from [22].

The first surgical simulator didn't make an appearance until 1868 when Dr. Benjamin Howard presented a lecture, "On the Radical Cure of Hernia". In this presentation he used a manikin to demonstrate a new hernia operation. Within two years of his presentation, the hernia simulator was a marketed product, selling for \$12. Shortly after this time, the U.S government published a study on the Medical and Surgical History of the War of the Rebellion. In one of the chapters on wounds to the abdomen, it was noted that intestinal suturing "should not be attempted on the living subject until the operator has acquired some experience by practicing...either using the fingers of a glove, or, better still...on intestines placed in a manikin" [23]. While they might not have realized it at the time, the U.S. government was well ahead of the curve, advocating for surgeons to use structured practice as the means for acquiring surgical skill.

### Deliberate Practice:

Although the psychology of adult education is an entire field in its own right, I will briefly delve into this topic and illustrate its importance as it pertains to surgical residency education and acquiring surgical skills. To begin, it is important to understand the process of learning a new skill. In their widely cited work, “Human Performance”, Fitts and Posner establish three phases of learning that one goes through in developing a skill. The first phase is referred to as the Early or Cognitive Phase. In this stage the learner is simply trying to “understand the task and what it demands” [24]. Learning can typically be done through instructions and demonstrations by a teacher at this point. The second phase is referred to as the Intermediate or Associative Phase. In this stage, the learner is trying to piece together some of the individual “chunks” of knowledge that they acquired in the early phase in order to build new patterns. It is the piecing of the smaller units into larger patterns when errors are often slowly eliminated from practice. The third phase is referred to as the Autonomous Phase. In this stage, much of the cognitive processing that was required for individual tasks in earlier stages becomes autonomous, “less directly subject to cognitive control, and less subject to interference from other ongoing activities or environmental distractions”. [24] In other words, the task requires little to no thinking as the behavior has become more natural.

Understanding these phases of learning is key to understanding how expert performance can be achieved because it helps to highlight where deliberate practice occurs on the spectrum of learning. To define deliberate practice, Ericsson et al suggest several criteria that must be met. They state that “the task should take into account the preexisting knowledge of the learners... The subjects should receive immediate informative feedback and knowledge of results of their performance. The subjects should repeatedly perform the same or similar tasks” [25]. This

concept of using feedback to improve performance aligns with the cognitive and associative stages laid out by Fitts and Posner. Ericsson et al expand on this idea by suggesting that expert performers are continually using these stages of learning in order to improve their craft as shown in Figure 2.

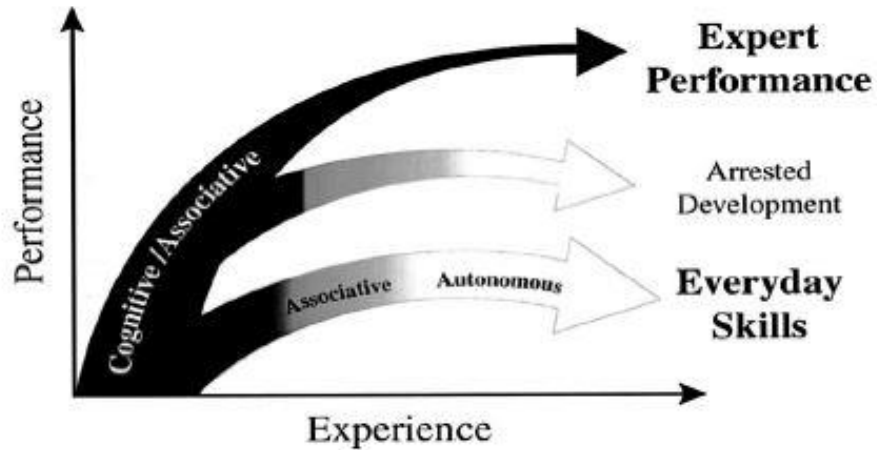


Figure 2 - An illustration of how expert performers are constantly learning and relearning their craft. Entering into the autonomous phase of learning can lead to what is described as “arrested development” [26].

In combination with deliberate practice, it has been shown that increased repetition of a task improves one's ability to perform that task. Ericsson et al state that “the amount of time an individual is engaged in deliberate practice activities is monotonically related to that individual’s acquired performance” [25]. This statement is further defended through the examination of the behavior of violin performers, from average players to professionals. Figure 3 displays a clear difference between the amounts of time spent practicing by a teacher, who might be considered an average violinist, and a professional. Not surprisingly, professionals have practiced for almost twice the amount of time as teachers by the time they are 20 years old.

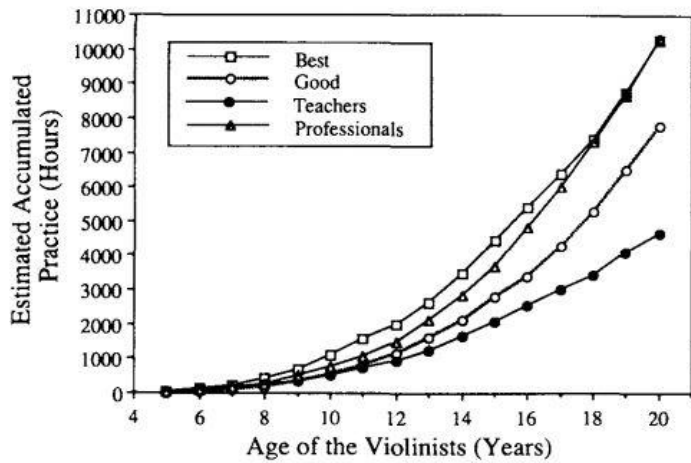


Figure 3 - A chart illustrating the difference between hours of practice by varying levels of skilled violin players. Graphic taken from [25].

These concepts of repeated deliberate practice are integral to the development of technical competency in the realm of orthopaedic surgery. Emphasizing the need for feedback in his examination on the development of motor skills in orthopaedics, Dr. Joseph Kopta notes that “there is little benefit and great potential harm for a learner to practice and not know whether or not he is performing correctly, and if not, what must be done to remedy the situation” [27]. Essentially, Dr. Kopta is arguing that not only will a surgeon not improve without feedback, but that there is the potential for developing poor skills with incorrect motor habits.

Correctly scheduling deliberate practice is another component that influences skill acquisition. A study by Moulton et al examined the difference between practicing in a large chunk of time or spreading out the practice over the course of several weeks. In the study, thirty-eight surgical residents were assigned to either a massed 1 day practice session or distributed weekly practice sessions. All groups were assessed before training, immediately after training, and 1 month after training to examine skill retention. The main finding of this study was that

although both groups performed at the same level immediately following training, the group that had distributed practice performed significantly better on the test 1 month after training [28].

This study illustrates that distributing practice over a period of time can lead to deeper skill development and skill retention.

Though previously defined in Ericsson's work, McGaghie et al. expand on the definition of deliberate practice and establish nine essential elements. In this paradigm, deliberate practice involves; highly motivated learners with good concentration, well defined learning objectives or tasks, an appropriate level of difficulty, focus and repetitive practice, rigorous and reliable measurements, information feedback from educational sources, monitoring and error correction, evaluation and performance that may reach a mastery standard where leaning time may vary but expected minimal outcomes are identical, and advancement to the next task [29]. In this work, McGaghie et al. perform a meta-analysis comparing deliberate practice using simulation-based techniques and the apprenticeship-training model. After examining 14 studies, the authors conclude that "without exception and with very high confidence, the CER data favor SBME [simulation-based medical education] with DP [deliberate practice] in comparison with traditional clinical education or a preintervention baseline measure" [29].

If we want today's surgeons to achieve an expert level of performance, providing an environment for deliberate practice is essential. The current paradigm of the apprenticeship model does not allow for deliberate practice. Incorporating simulation into the model of surgical education will provide this needed space.

### Simulation in Laparoscopic Surgery:

Laparoscopic surgery is an excellent example of how beneficial practicing in a simulated environment can be. This type of surgery is a very complex procedure that involves coordinating cameras (laparoscopes) and various hand held instruments in a confined space [30]. When performing a laparoscopic cholecystectomy, a procedure to treat symptomatic gallbladder diseases [31], common surgical complications can include perforation of the bowel or bladder, bleeding of the abdominal wall, and injury to the common bile duct [32]. When this procedure was first accepted by the surgical community, initial reports indicated that complication rates for the closed laparoscopic procedure might be higher than those of the previously more conventional open procedure [12]. Zucker et al noticed that there was a lack of training available at the time and postulated that having more “hands-on clinical training would reduce the risk of biliary tract complications that were often being reported from institutions that had initiated laparoscopic surgery without the benefit of experienced instruction” [33].

In 1998 the McGill Inanimate System for Training and Evaluation of Laparoscopic Skills (MISTELS) was developed [34]. The MISTELS system is a laparoscopic simulator that allows surgeons to use operative tools to practice various techniques that might be used during a laparoscopic procedure. The trainer consists of seven exercises that were designed to both develop laparoscopic coordination skills, emphasize the use of certain instruments, and focus on particular laparoscopic techniques [34]. This system became widely accepted and has helped to demonstrate how effective training on a simulator can be. An image of the MISTELS system can be seen in Figure 4.

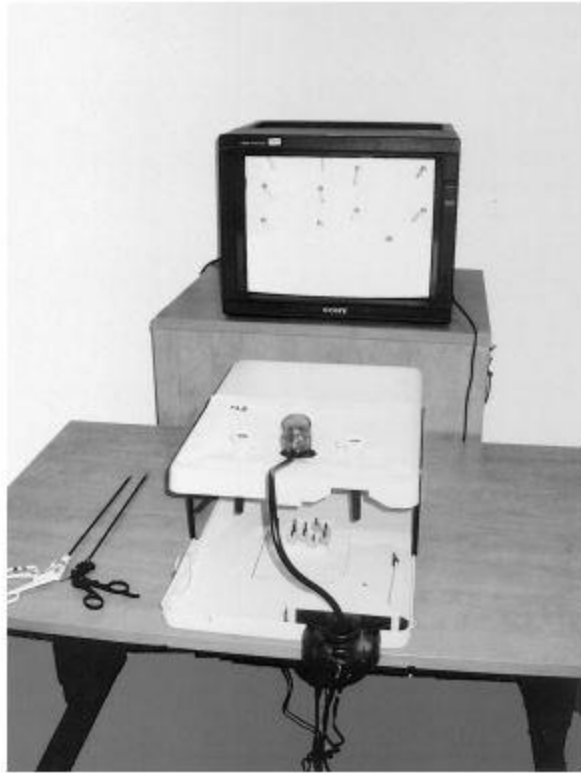


Figure 4 - An image of an early development of the MISTELS system. Image taken from [35].

A study performed by Fried et al. aimed to prove the value of the MISTELS system in training surgeons. In the experiment, 200 surgeons of varying levels of experience were recruited to train on the different exercises of the simulator. In examining the construct validity of the simulator, or the ability to discriminate between varying levels of expertise [36], the study found a significant difference between junior, intermediate, and senior level surgeons on all tasks. In examining concurrent or predictive validity, that is “the relationship between scores obtained in the MISTELS and laparoscopic technical skills measured in a live operating room” [35], a high correlation was observed that was also found to be statistically significant ( $P < 0.001$ ). This study begins to illustrate the validity of the MISTELS as both a training and assessment tool.

Several studies have examined how training with this system translates into performance in the operating room. In a study by Sroka et al, nineteen residents were enrolled in a training program using the MISTELS system to examine how their performance in the operating room would change. The residents were split into a control group (n=9), which did not train with the simulator, and a training group (n=8). Both groups were assessed prior to any training and it was found that there was no difference between the groups in either the OR environment or in the simulated environment. However, after completing the training, the group that practiced with the simulator showed significantly better scores in both the OR and with the simulator. It is worthy to note that both the control and training group did experience some level of improvement in the OR, however the training group showed significantly greater amounts improvement ( $P<.0001$ ) [37]. This study clearly demonstrates the impact that training in a simulated environment can have on improving performance in the OR.

Skill retention is another way to assess how well a task has been learned or acquired. Mashaud et al. enrolled 91 surgical residents in a study to investigate how skill was retained over a 2 year period after undergoing a proficiency based training program on the Fundamentals of Laparoscopic Surgery (FLS). The FLS utilizes the MISTELS simulator and was introduced in 2004 by the Society of American Gastrointestinal and Endoscopic Surgeons and subsequently became a requirement of the American Board of Surgery for taking written board examinations [38, 39]. After training to proficiency on the FLS, residents were asked to retest on two of the tasks every 6 months for a 2 year period. If the resident was found to be performing below levels of proficiency during a 6 month retest, the resident would retrain until two consecutive attempts were made at proficient levels of performance. The results of this study showed that as residents were trained and retrained, proficiency levels continued to rise over the course of the two year

period. The most convincing result from this study perhaps was that at the end of the two year period, 20 year 4 and year 5 residents took the certification exam and had a 100% pass rate, compared to the initial test 2 years prior where only 8 of the residents would have passed [40].

There are many more studies illustrating the success that the laparoscopic community has had in utilizing simulation based training to improve the performance of their surgeons [41-43]. However, the point is clear after examining a few studies that training in a simulated environment can greatly improve one's performance and that this improvement can be seen when transferred to the operating room.

#### Simulation in Orthopaedics:

Despite the large amount of evidence supporting simulation-based education in many surgical fields, orthopaedics has been slow to adopt this model into its training. Much of the progress that has been made in orthopaedics is within the domain of arthroscopic surgery, a procedure that draws many parallels to laparoscopic surgery. However, in a review of arthroscopic training published in 2014, only 14 articles were found that had been published on simulation training in this field [36]. The main purpose of this article was not to illustrate the lack of research currently present in orthopaedics; however it is clearly lacking when compared to the more than 200 publications on laparoscopic surgery simulation published between 1992 and 2009 [44].

Perhaps one of the barriers to entry for orthopaedics thus far has been simulation cost. In a 2011 survey of residency directors, 87% of directors said that a lack of available funding was the most substantial barrier to the development of a formal surgical skills program [45]. Additionally, 62% of respondents said that they would be willing to pay between \$1000 and

\$15,000 for a surgical simulator. Unfortunately, many of the simulators available today in orthopaedics use expensive technologies, such as haptic feedback [46]. These technologies can be very expensive and cost upwards of \$100,000, well above the price range of most residency programs [47].

With that in mind, some of the recent success that has been observed in orthopaedics has been with lower cost simulation modules. In a manner similar to the Fundamentals of Laparoscopic Surgery, Lopez et al. developed series of stations that they refer to as the Fundamentals of Orthopaedic Surgery (FORS) [48]. The FORS is an orthopaedic skills board that was made from supplies that can be purchased at local hardware stores for less than \$350 (Figure 5). It contains six modules which are intended to assess different psychomotor skills such as fracture reduction, three-dimensional drill accuracy, simulated fluoroscopy-guided drill accuracy, depth-of-plunge minimization, drill-by-feel accuracy, and suture speed and quality.

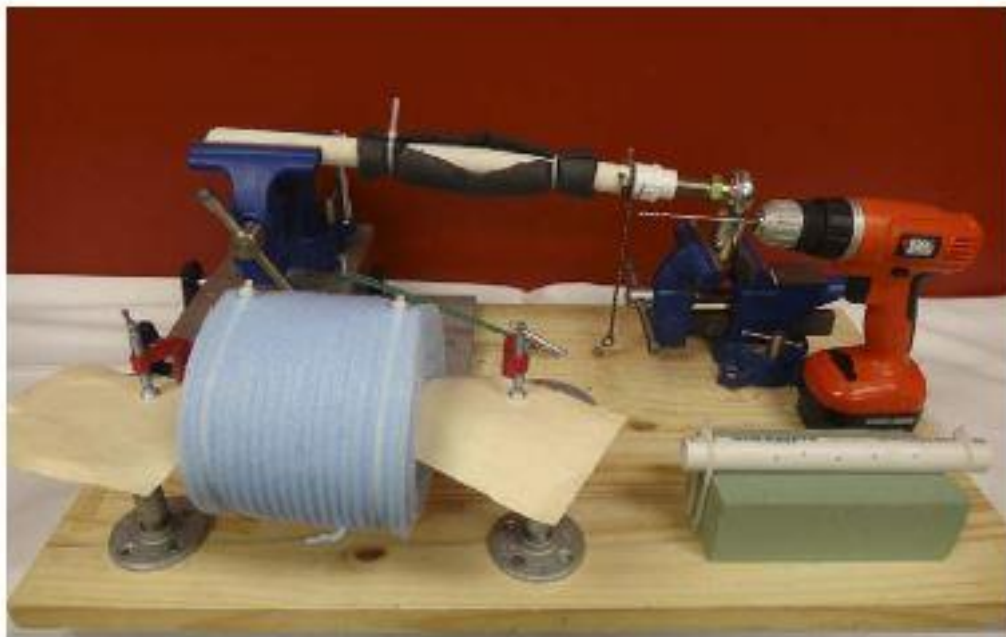


Figure 5 - The FORS skill board containing six stations to assess different orthopaedic skills.

In the study involving the FORS system, 47 medical students, 58 orthopaedic surgical residents, and 29 attending physicians were tested on the modules, with medical students being retrained to examine their improvement. The results of the study showed both that the FORS could distinguish between medical students, junior residents, and attending physicians, and that with practice, the medical students could achieve significant levels of improvement.

Another example of using low cost tools to train and assess orthopaedic residents is the Bonedoc DHS simulator. This simulator is a virtual reality environment run on a PC computer that allows a user to position a virtual x-ray machine at their discretion, reduce a fractured hip, and place a lag screw in the femoral neck of the virtual patient (Figure 6). In a study by Blythe et al, three groups of students, medical students, basic trainees, and advanced trainees, all perform six virtual operations with the Bonedoc simulator. Although the study had a small number of participants ( $n=18$ ), the results were able to discriminate between the novice and expert trainees across several metrics of performance [49].

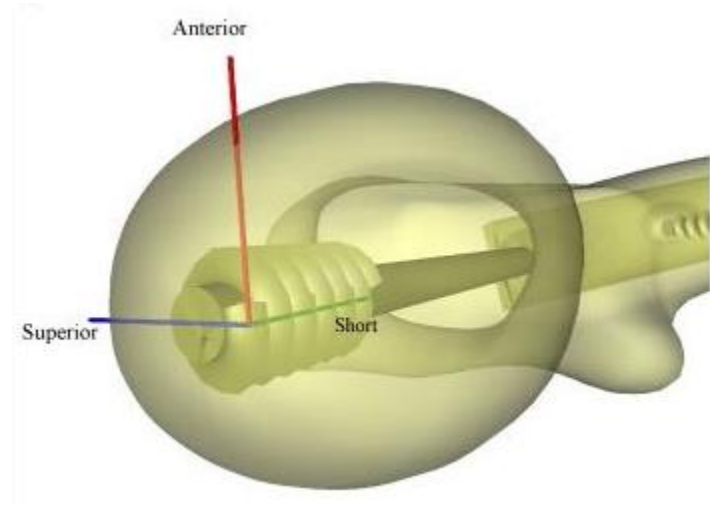


Figure 6 - An image of a lag screw being placed inside the virtual bone in the Bonedoc DHS simulator. Image taken from [49].

The study by Blyth et al. is an interesting and somewhat unique study because it uses clinically relevant measurements to assess performance of the user, such as the number of X-rays used, the placement of the implant, and the total amount of surgical time to complete the procedure [49]. Most other studies that assess performance on a simulator use an objective scoring system known as the Objective Structured Assessment of Technical Skills (OSATS) to assess performance [50]. The OSATS metric is a combination of scores from several different categories aimed at assessing surgical performance such as the surgeon's respect for soft tissues, instrument handling, flow of operation, and knowledge of specific procedure [50]. This form of performance assessment has been heavily studied and validated and is a relevant way to measure some aspects of surgical performance. However, recent studies have shown that clinical outcomes may not be correlated with the OSATS metric and therefore may not provide a complete picture of surgical performance [51, 52]. In other words, these studies suggest that a surgeon may perform the procedures of an operation with technical proficiency, but produce results that are not equally positive in a clinical sense. Therefore, it is important that future studies examining surgical performance not only provide an OSATS metric of surgical performance, but also a clinically relevant form of measurement.

#### Simulation in Hip Fractures:

Hip fractures are an area of major concern in the world of orthopaedics. Each year there are at least 250,000 adults age 65 and older in the United States who are hospitalized for a hip fracture [53]. It is reported that roughly 30% of people with a hip fracture will die within a year of the incident [54]. Given that this event occurs mainly in the elderly patients, with the aging population of the United States, this problem is only bound to grow. A study by Schneider et al. estimated that by the year 2040, the annual incidence of hip fractures will increase to more than

500,000 cases each year [55]. Given the seriousness of this issue, it is critical that the adequate training in the treatment of hip fracture patterns is available to orthopaedic residents so that they can successfully administer treatment as physicians.

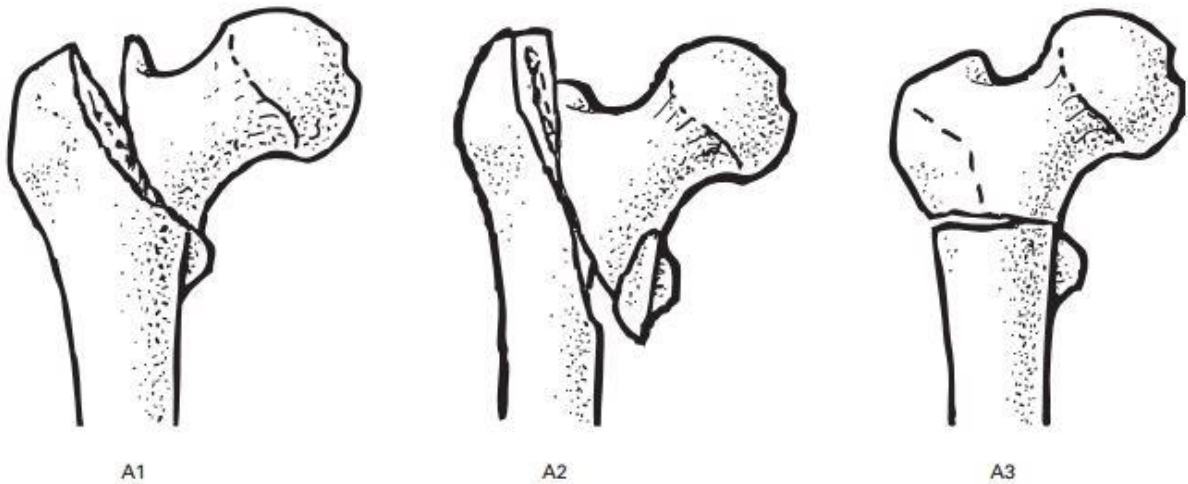


Figure 7 - Graphics depicting the three categories of intertrochanteric hip fractures. Image taken from [56].

Depending on the type of hip fracture presented to a surgeon, different treatment options are available. For the purpose of this discussion, we will focus on intertrochanteric fractures (Figure 7). An intertrochanteric fracture “occurs between the neck of the femur and a lower bony prominence called the lesser trochanter” [57]. Although there can be some debate among surgeons, the conventional form of surgical treatment for this type of fracture pattern involves implanting a dynamic hip screw (DHS) across the line of the fracture and into the femoral head of the femur [58] (Figure 8). Prior to implanting the DHS into the femoral head, a guide wire is first implanted in the same intended position as the final implant will be in. Placing this guide wire is one of the critical components to this surgical procedure because it will dictate where the final implant is placed in the bone.

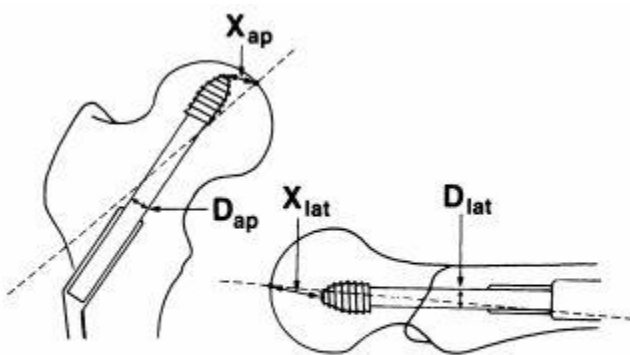


Figure 8 - Radiographic images showing an implanted dynamic hip screw. In some cases an additional screw is added superiorly to provide additional stability to the fracture. Image taken from [59].

Placing the guide wire into bone is a common orthopaedic procedure known as wire navigation. Wire navigation involves using radiographic images from different viewpoints to create a 3D model of the patient's anatomy and understand where your tools or implants are relative to that model. This procedure is complex and difficult to master because it involves interpreting sets of 2D images and translating that data mentally into a 3D scene. In placing a guide wire for an intertrochanteric fracture, the two viewpoints commonly used are called the Anterior-Posterior (AP) and Lateral views (Figure 9).

In their widely cited paper, "The Value of the Tip-Apex Distance in Predicting Failure of Fixation of Peritrochanteric Fractures of the Hip", Baumgaertner et al. show how the placement

of a DHS in the femoral head of the femur can have a large impact on the outcome for patients after surgery. In the study, Baumgaertner develops a metric referred to as the tip-apex distance (TAD) that describes how far the tip of the implanted screw is from the apex of the femoral head (Figure 9). The results of this study clearly indicate that for implants with a post-operative TAD of less than 25mm, the likelihood of the implant “cutting out of the femoral head”, or failing, is significantly less ( $P = .0001$ ) than implants who had a TAD greater than 25mm [60].



$$TAD = (X_{ap} \times \frac{D_{true}}{D_{ap}}) + (X_{lat} \times \frac{D_{true}}{D_{lat}})$$

Figure 9 - This image describes the calculation of the TAD. It is a sum of the distances in both the anterior-posterior and lateral views. Image taken from [60].

Because the tip apex distance is both easily measured and a clinically relevant metric, the surgical procedure of repairing an intertrochanteric hip fracture lends itself to assessment with a surgical simulator. As was mentioned before, Blyth et al. have introduced a virtual reality application that allows users to practice the steps of this technique. However, there is a large gap between using a computer to visualize the virtual fixation of a fracture and actually using a drill and surgical instruments to repair a patient’s anatomy. Swemac, a European implant company, has developed a surgical simulator called *TraumaVision* that is designed to allow surgeons to

practice this procedure and understand the feeling of drilling into bone [61]. However, this simulator uses haptic feedback to provide the sensation of drilling into bone and is therefore a very expensive product for surgical residency programs to purchase.

Thomas et al. recently developed a hybrid reality simulator that had great potential for training residents in the task of hip wire navigation. This simulator combined real world objects, such as a synthetic bone and a surgical drill, in combination with an electromagnetic tracking system to generate virtual radiographic images [62]. This simulator was a novel idea because it provided residents with the ability to practice placing the guide wire using the same instruments used in the operating room and receiving the same types of radiographic images, but without exposure to any radiation. Unfortunately, the main component that allowed the simulator to function, the electromagnetic tracking device, was very expensive and would have been at the limits of most residency program budgets. Although a promising tool, this simulator is not available on the market for residency programs to use.

Despite some limitations of the hybrid reality device developed by Thomas et al, their initial work showed that training on this type of platform had great potential. In a study that involved 40 participants, it was shown that the simulator could distinguish between novice and expert performance [63]. It was additionally shown that the novice group could achieve significant improvement in their performance when training on the simulator. These results indicate that this type of platform could be very beneficial in training resident surgeons.

For surgical residency programs looking to incorporate the skills of hip fracture repair into their curriculum, there are currently very few options available. Although proficiency in treating hip fractures is one of the orthopaedic surgery milestones defined by the Accreditation

Council for Graduate Medical Education (ACGME), little work has been done to develop tools that can aid in the training of resident surgeons on this task. Certainly, a skills program could use cadavers and fluoroscopic units to practice this type of procedure; however that can both be expensive and potentially harmful to the residents due to the radiation exposure from the fluoroscopic images that would be taken during practice. Furthermore, in a survey of surgical skills labs across the U.S, only 22% reported having a C-arm (fluoroscopic unit) available [45].

#### Summary:

Surgical simulation has been proven to be an effective form of training surgeons outside of the operating room. Orthopaedics has been a field that has lagged behind adopting this new training paradigm. However, as technical skills training has become a requirement for first year residents, programs are beginning to adopt simulation into their teaching curriculums [64]. This work will center on the development of a surgical simulation tool for training residents in the task of wire navigation for hip fractures. It aims to create an affordable tool that will give orthopaedic residents the ability to safely and deliberately practice the skill hip wire navigation.

## **Chapter 2: Simulator Design**

### Introduction:

This chapter will focus on the work that has been done in developing a surgical simulator for the task of hip wire navigation. Design parameters are laid out initially to help frame the needs that this simulator is intended to fill. An initial design of the simulator is then presented, covering both the hardware and software components of the design. Following field testing and some intermediate results, a second design iteration was performed to improve the simulator performance. The hardware and software components of this second iteration will be presented, followed by the steps taken to assess the second iteration of the simulator.

### Simulator Design Parameters:

Given the complex nature of orthopaedic surgery, or surgery in general, it is doubtful to think that a simulator will be able to recreate every aspect of a procedure. Instead, it is more important to focus on the key components of a particular surgery and analyze what tools will be best suited in helping a learner overcome the challenges of a procedure. For example, the MISTELS system, which has had enormous success, is a relatively low-tech training tool that does not attempt to recreate every component of a laparoscopic cholecystectomy. Instead, it focuses on different key elements of the procedure that combine to form a powerful training platform. Additionally, it uses the same surgical instruments that are used in the operating room so that when the surgical skills are mastered on the simulator, they easily translate into a clinical environment.

In the realm of hip wire navigation, there are several elements that are key to gaining a mastery of the procedure. First is having an understanding of the radiographic images that are

presented to the surgeon. In the procedure of placing a guide wire across an intertrochanteric hip fracture, the ultimate goal is to place the guide wire within 25 mm of the apex of the femoral head. In order to do so successfully, a surgeon must use radiographic images provided during surgery to place the guide wire. As was mentioned earlier, AP and lateral images of the patient's anatomy help surgeons understand the 3D relationship between the guide wire they are placing and the patient in front of them. One of the hardest parts of this procedure is in gaining an appreciating for how to move the guide wire in either image plane to correctly position the implant in bone. Therefore, providing AP and lateral images of where a guide wire is relative to bone is an essential component that must be incorporated into a surgical simulator for the task of hip guide wire navigation.

Another important component of the procedure is being able to feel the different densities of bone when drilling in the guide wire. In trying to place the guide wire near the apex of the femoral head, the implant can come very close to the boundary of the bone cortex. In order to prevent the guide wire from breaching the cortex and entering into the joint space of the patient, a surgeon must be able to feel the density change in bone as they move closer to the cortex (Figure 10). Breaching the cortical wall and entering into the joint space could potentially be harmful to the patient and should be avoided at all costs. For these reasons, it is critical that the simulator provide users with a similar somatosensory feedback that would be achieved when drilling into bone.

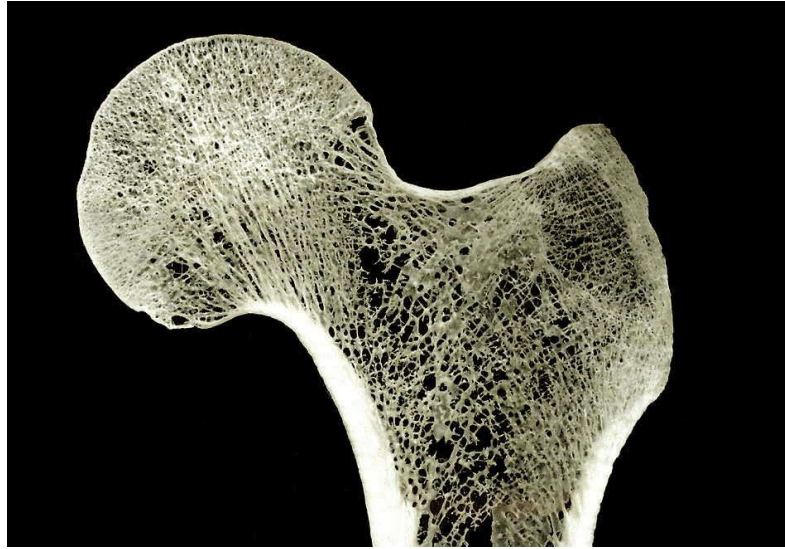


Figure 10 - A cross section of a proximal femur illustrating the changes in bone density depending on the location in bone. Image taken from [65].

The remaining design parameters for this simulator are that it incorporates the same surgical instruments that are used in the OR, mainly a guide wire and a guide wire driver, and that the simulator is designed with a technology that will be affordable to residency programs. The hip simulator that was previously mentioned, *TraumaVision* did not use the surgical instrument used in the OR in its system. Instead, it uses haptic technology to provide the user with an image of virtual guide wire and virtual guide wire driver. The virtual guide wire driver is controlled by a wand that is suspended in mid-air relative to a virtual femur. When the user moves this wand toward the virtual bone and contact is made, a feedback of vibration is sent back to the user, in an attempt to tell them they are touching bone. Similarly, when a button on the wand is pressed, a vibrational feedback of drilling is presented to the user. Unfortunately, given limitations in the technology of haptics, there is much that is left to be desired when using this system. Detecting different densities of bone is very difficult and simply knowing where one's virtual guide wire is relative to the virtual bone can be quite confusing. Furthermore,

haptics are an expensive technology and the *TraumaVision* product has been quoted to cost as much as \$90,000, well above the budget of most residency programs [45, 47]. For these reasons, it is apparent that using a real guide wire and guide wire driver in accordance with a technology to track the instruments relative to a fixed bone will create a more effective and affordable tool for training residents. In this application, computer vision principles will provide the capability to track the guide wire as it is drilled into bone. The following sections of this chapter will go into detail on how computer vision principles were adapted for this application.

#### Simulator Conceptual Overview:

Before going into the specifics of the simulator design, I will first provide an overview of how the simulator is intended to function. There are two main components to the system; the simulator hardware and the simulator software. These entities interact with one another to provide both the physical platform for which a resident is operating on and to create/display the artificial or virtual radiographic images of the guide wire that is being inserted into bone. In laying out the system hardware, the main components are two mounted cameras, a rigidly fixed synthetic proximal femur that is covered to occlude the bone anatomy from the user, a guide wire, a guide wire driver, and a laptop.

A resident will typically begin the simulation by palpating the bone anatomy to find their starting point for the guide wire. When a resident is satisfied with the starting point, he or she will request either an AP or Lateral image. At this point, the cameras, which are positioned at orthogonal views to the workspace of the resident, will acquire images of the current position of the guide wire. These images are then sent through a series of image processing steps. The goal of the image processing is to acquire two main pieces of data; the vector of the wire relative to

bone and where the tip of the wire lies along that vector. Once these values are known, the wire can be projected into bone and a virtual radiograph is displayed to the resident. The resident will then use the information from the virtual image to adjust the position of their guide wire. As adjustments in guide wire position are made, the resident will continue to request virtual images, from either the AP or Lateral view. This cycle of adjusting wire position and requesting images will continue until the resident is satisfied with the placement of the guide wire, at which point, the simulation session is complete. A schematic diagram laying out this process can be seen in Figure 11.

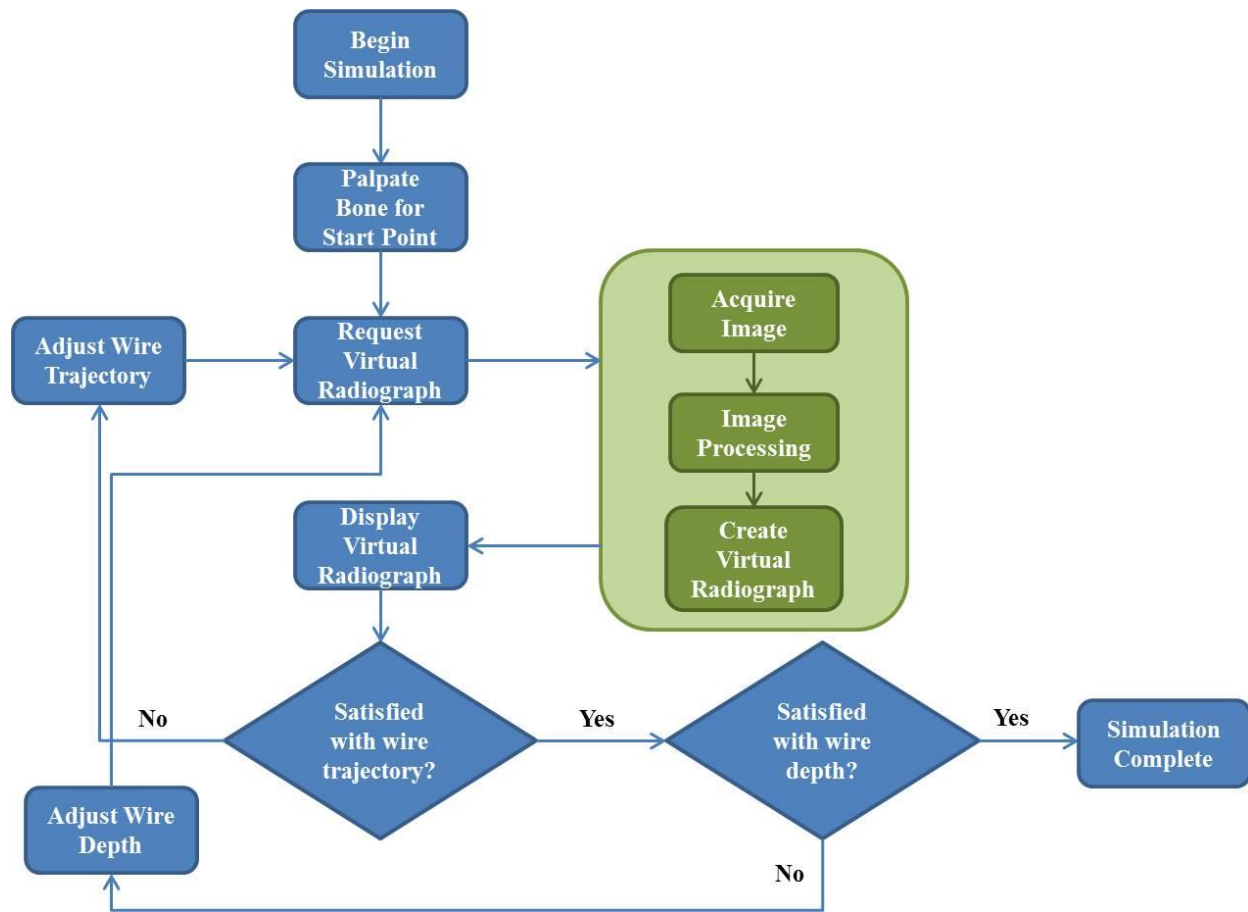


Figure 11 - A schematic diagram depicting the flow of data when using the simulator.

In order to calculate the 3D vector of the guide wire, the scene must first be calibrated. The calibration technique used for this system is the Direct Linear Transform (DLT). This is a commonly used technique in computer vision applications that involves matching known 3D coordinates of points on a calibration target with corresponding 2D points in a pair of orthogonal images of the calibration target [66-68]. Work done by Abdel-Aziz et al. has illustrated that a linear transform can be calculated to move between the 3D coordinate space of an object of interest and two 2D images of that object.

To further explain how the linear transformation occurs, begin by considering a calibration object of some nominal geometry placed inside a coordinate space (X, Y, Z). This defines the object space reference frame. Then consider two cameras placed orthogonally in the direction of the cube. The coordinate space for the image frames of these cameras can be defined as ( $U_L, V_L$ ) and ( $U_R, V_R$ ) for the left and right cameras. An initial assumption is made that we know the location of a point on the calibration object (X, Y, Z). When the object is imaged by the left and right cameras, the known point on the target object can be found in both images as the points ( $U_L, V_L$ ) and ( $U_R, V_R$ ). The image coordinates can then be related to the object coordinates through a series of constants as seen below:

$$U_L = \frac{L1 * X + L2 * Y + L3 * Z + L4}{L9 * X + L10 * Y + L11 * Z + 1} \quad (1)$$

$$V_L = \frac{L5 * X + L6 * Y + L7 * Z + L8}{L9 * X + L10 * Y + L11 * Z + 1} \quad (2)$$

$$U_R = \frac{R1 * X + R2 * Y + R3 * Z + R4}{R9 * X + R10 * Y + R11 * Z + 1} \quad (3)$$

$$V_R = \frac{R5 * X + R6 * Y + R7 * Z + R8}{R9 * X + R10 * Y + R11 * Z + 1} \quad (4)$$

From these equations it can be seen that when relating one calibration point between the object coordinate frame and the image coordinate frame there are 7 known variables ( $X$ ,  $Y$ ,  $Z$ ,  $U_L$ ,  $V_L$ ,  $U_R$ ,  $V_R$ ), 22 unknown variables ( $L_1$  through  $L_{11}$ , and  $R_1$  through  $R_{11}$ ), and only 4 equations. Linear algebra principles remind us that to solve for the 22 unknowns, we will need at least 22 equations. Given that each new point on the cube provides four equations, in order to solve for the 22 unknown  $L$  and  $R$  parameters, there must be at least 6 known target points on the calibrations, creating a system of 24 equations. The equations for the left image parameters and right image parameters can both be rearranged into a system of equations with matrices as seen below in Figure 12.

$$\begin{array}{l}
 \text{Point 1} \\
 \text{Point 2} \\
 \vdots \\
 \text{Point } N
 \end{array}
 \left\{
 \begin{array}{c}
 \left[ \begin{array}{ccccccccc}
 x_1 & y_1 & z_1 & 1 & 0 & 0 & 0 & -u_{L1}x_1 & -u_{L1}y_1 & -u_{L1}z_1 \\
 0 & 0 & 0 & 0 & x_1 & y_1 & z_1 & 1 & -v_{L1}x_1 & -v_{L1}y_1 & -v_{L1}z_1 \\
 x_2 & y_2 & z_2 & 1 & 0 & 0 & 0 & -u_{L2}x_2 & -u_{L2}y_2 & -u_{L2}z_2 \\
 0 & 0 & 0 & 0 & x_2 & y_2 & z_2 & 1 & -v_{L2}x_2 & -v_{L2}y_2 & -v_{L2}z_2 \\
 \vdots & & & & & & & & & & \\
 x_N & y_N & z_N & 1 & 0 & 0 & 0 & -u_{LN}x_N & -u_{LN}y_N & -u_{LN}z_N \\
 0 & 0 & 0 & 0 & x_N & y_N & z_N & 1 & -v_{LN}x_N & -v_{LN}y_N & -v_{LN}z_N
 \end{array} \right] \\
 \underbrace{\quad\quad\quad}_{2N \times 11}
 \end{array}
 \right. = \left. \begin{array}{c}
 \left[ \begin{array}{c}
 L_1 \\
 L_2 \\
 L_3 \\
 L_4 \\
 L_5 \\
 L_6 \\
 L_7 \\
 L_8 \\
 L_9 \\
 L_{10} \\
 L_{11}
 \end{array} \right] \\
 \left[ \begin{array}{c}
 u_{L1} \\
 v_{L1} \\
 u_{L2} \\
 v_{L2} \\
 \vdots \\
 u_{LN} \\
 v_{LN}
 \end{array} \right] \\
 \underbrace{\quad\quad\quad}_{2N \times 1}
 \end{array} \right) \quad 11 \times 1$$

Figure 12 – A system of equations can be arranged to solve for the 11  $L$  and 11  $R$  image parameters. Image taken from [68].

Once these systems have been formed, the  $L$  and  $R$  parameters can be solved using the Moore-Penrose pseudoinverse method as seen in the two equations below. In the equation,  $L$  and

$R$  are the column matrices containing the unknown parameters,  $A$  is the  $2N \times 11$  matrix containing the known object coordinates, and  $B$  is the  $2N \times 1$  column matrix containing the known image coordinates.

$$L = (A_L^T * A_L)^{-1} * A_L^T * B_L \quad (5)$$

$$R = (A_R^T * A_R)^{-1} * A_R^T * B_R \quad (6)$$

Once these parameters have been calculated, the scene that the cameras are imaging is considered to be calibrated. These parameters can then be used to calculate the 3D locations of unknown points on an object in the scene given that there is a set of corresponding points from both sets of orthogonal images. In other words, if a feature can be found on an object in both the left and right images, the parameters can then be used to determine what the coordinates of that feature are inside the calibrated scene. In the context of imaging a guide wire, this technique is used to take feature points on the wire found in both images and calculate their 3D coordinates. When multiple feature points of the wire are found and back projected into 3D coordinates, this creates the vector of the wire relative to the fixed bone.

As was mentioned briefly earlier, after the vector of the wire is known relative to bone, the remaining degree of freedom to be calculated is where the tip of the wire sits along that vector. Essentially, this equates to knowing where the cameras are looking along the length of the wire. This piece of information is achieved through specifically designed markings on the wire which act as address locators. When an address on the wire is correctly identified, and it is known how far from the tip of the wire that address exists, then the distance which the wire tip should be projected along the vector of the wire can be determined. With this final piece

of information in place, the location of the guide wire can be properly projected into bone and a virtual radiograph can be generated.

Now that the underlying concepts of the simulator are understood, I will go into the details of two design iterations. In each design, both the hardware and software (image processing) components will be presented.

### Design Iteration 1:

#### Hardware Design:

The first iteration of the simulator can be seen below in Figure 13. In the initial design, two USB web cameras are mounted on adjustable brackets with the cameras positioned so that they are looking down on the workspace of the resident. LED lighting has also been mounted to the cameras so that there is always a strong source of light illuminating the guide wire that the cameras are focused on. A synthetic proximal femur purchased from Sawbones (model 1130-21-19, Sawbones Inc., Vashon WA, USA) is mounted to a rigid acrylic construct that holds the bone in place while the simulator is in use. The femur was mounted so that it sits with the femoral neck in a 15 ° angle of anteversion as is anatomically typical [69]. A sheet of black foam is wrapped around the Sawbones femur so that the particular anatomy of the femur is hidden from the view of the resident, as it would be in a normal surgery. Additionally, an incision along the black foam is been made prior to a resident using the simulator so that they focus entirely on the task of wire navigation.

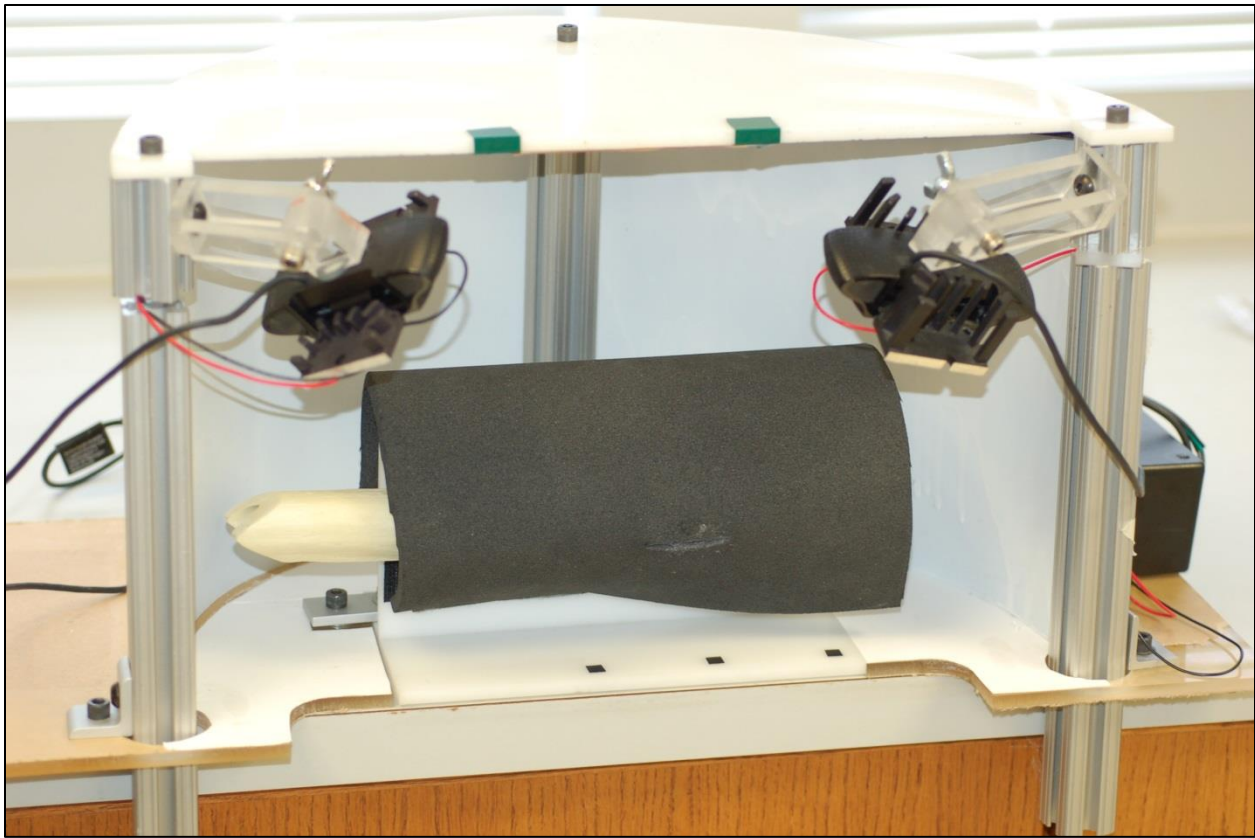


Figure 13 - A display of the first iteration of the wire navigation simulator. The laptop, guide wire, and guide wire driver are not shown in this image.

The acrylic construct that holds the femur also serves as the calibration object. Six thin black metal square pieces are cemented to the acrylic surface in a pattern surrounding the area in which the guide wire will likely be imaged. In designing a calibration object that will be used in a DLT algorithm, it is advised that the known calibration points be spaced so that they span the area of interest and that the region intended for imaging be contained within that area [68].

Placing the metal square pieces around the bone was intended to satisfy this constraint.

To place the calibration points and the proximal femur together in a known coordinate system, a laser scan of the bone mounted to the calibration object was obtained using a FaroArm laser scanner. The FaroArm is a flexible laser scanner that allows complex geometries to be

captured with an accuracy of 0.024 mm [70]. The laser scan was then imported into Geomagic, software designed to help in reverse engineering projects and registering objects to different coordinate systems. In Geomagic, the coordinates of the four corners of each square black tile were queried and recorded for use as the known points in the DLT calibration algorithm. A stereolithography (STL) file of the laser scanned bone was also exported so that it could be used in the creation of virtual radiographic images. With the coordinates of the calibration points and the femur model now aligned to the same coordinate system, calculations of the guide wire location relative to bone could be accurately made. An image of the laser scanned bone and calibration object can be seen in Figure 14.

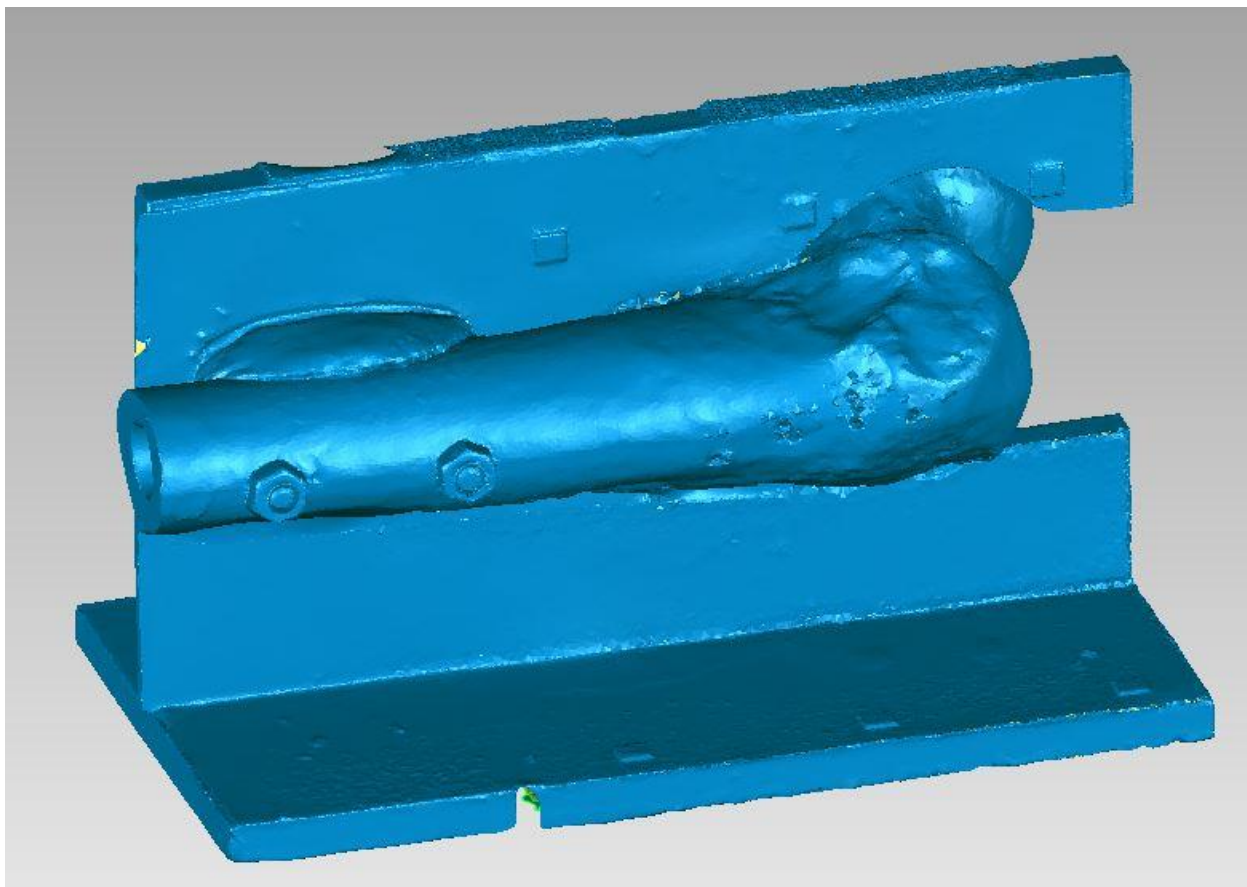


Figure 14 - The laser scan of the proximal femur mounted to the calibration object.

Another important feature of the hardware was the design of the guide wire. The guide wire is one of the most important features because all of the image processing that is done to generate the virtual radiographs is centered on locating feature points of the guide wire. In designing the feature points, a line sequence was developed and laser etched in black onto the wire. The sequence was designed so that along the length of the wire, different discrete regions would represent different line addresses. Each address of the wire is an 8mm length of wire. Addresses are then separated by a 2.5mm thick black line that acts as either the end of one address or the beginning of another address. In between these start/stop points, lines of varying thickness (1mm or 1.5mm) are placed at incremental locations from the start of the address. For instance, the second address is a 1mm thick line spaced 2mm from the start of the address. The third address is the same, but the 1mm line is spaced at 3mm from the start of the address. As the wire progresses, the addresses become more complex, sometimes with two 1mm lines and sometimes with both a 1mm line and a 1.5mm line. The addresses were designed with the intention that if two addresses were imaged next to one another, they would be unique enough to distinguish from two other addresses located along the wire. An image of the laser etched guide wire can be seen in Figure 15.



Figure 15 - The wire address scheme is shown here. Addresses are separated by a 2.5mm thick line.

## Software Development:

The software developed for this simulator was completed using Matlab. The first step in running the software is to calibrate the cameras in reference to the coordinate frame of the Sawbones femur. The calibration step is a manual process that requires a user to select the corners of each square on the calibration target in images from both the left and right cameras. Once these points have been selected, a Matlab script calculates the left and right image parameters using the system of linear equations previously discussed. These parameters are then stored as variables until they are later used to reconstruct the vector of the guide wire.

Once the scene has been calibrated and a Sawbone femur has been fixed to the simulator base, an image of the blank scene, meaning no guide wire is present, is taken by each camera. This blank image is stored and used in one of the first image processing steps taken to isolate the guide wire in the image. When a resident begins the simulation, the cameras are initialized by the Matlab software and placed in a continuous capture mode. At the moment a resident requests an AP or lateral image, the software grabs the most recent image of the scene from each camera. The acquired images from each camera then goes through a series of image processing techniques in order to calculate both the 3D vector of the guide wire its projection along this vector. The image processing can be broken down in to three main steps; gross edge detection, fine edge detection, and address assessment.

The first image processing step begins by subtracting the most recently acquired image of the scene from the blank image captured before starting the simulation, creating a difference image. Although there may be some extraneous noise present due to a change in external lighting conditions, this first step does a good job of isolating the wire in the image.

The difference image is then converted to a black and white binary image. The threshold for the binary conversion is found using the method developed by Nobuyuki Otsu. In this method, the threshold value is optimized so that the between-class variance is maximized [71]. Once the binary image is created, it is then turned into an edge image using the Canny edge detection method. The Canny edge detection method is a very well-known and often used methodology for edge detection because it achieves such good results. This method was first developed by John Canny in 1986 as part of his graduate work. Without going into great detail, the method works by going through four main steps; Gaussian smoothing to remove image noise, creating an intensity gradient image, applying non-maximum suppression, and thresholding with hysteresis [72]. The results of the canny edge detection can be seen below in Figure 16.

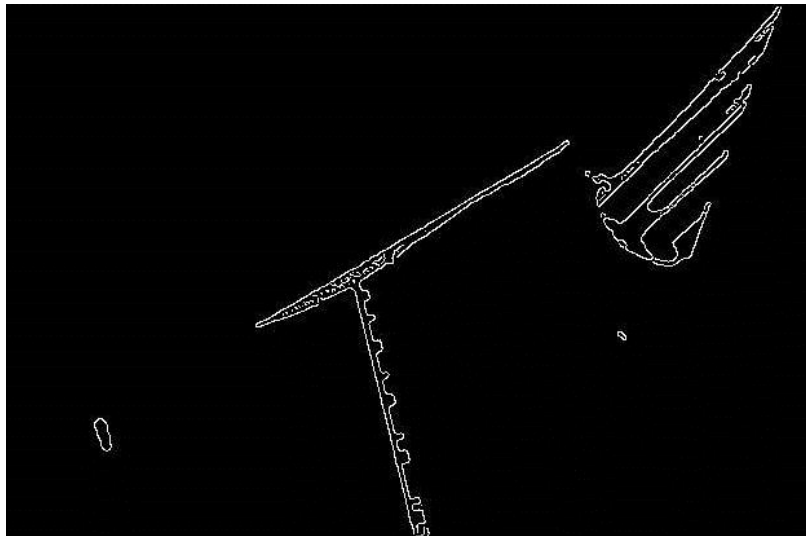


Figure 16 - The results of the edge detection on the left image are shown here. It is noticeable that one side of the wire has a clean edge to it while the other side has missing gaps that were missed in the edge detection.

Once the edge image has been created, the next step is to find the lines in the image which define the outside edges of the guide wire, or the edges that run along the length of the

guide wire. In order to find these lines, the image is taken through a Standard Hough Transform. The Hough Transform is a powerful technique which takes a point in an image ( $x, y$ ) and transforms it into an array of lines in what is commonly referred to as the Hough space [67]. In the Hough space, a point is then defined by an angle value ( $\theta$ ) and the perpendicular distance from the origin at which that line could potentially sit in the image space ( $\rho$ ). This means that in the image space, a line may have been defined as a series of collinear points, however, in the Hough space, a line is defined when there is an intersection of many potential lines at one particular  $\rho$  and  $\theta$  value. The equation for the transformation from the image space to the Hough space can be seen below.

$$\rho = x * \cos(\theta) + y * \sin(\theta) \quad (7)$$

Once the Hough transform has been completed, the strongest edge of the wire is found first by locating the strongest peak of intersecting lines in the Hough space. After this peak is located, the Hough space is then filtered so that only potential lines parallel to this first line remain viable. Given that we are looking for the outside edges of the wire, it is safe to assume that the two lines which define these edges will be parallel. A search is done to the left and right of the first wire edge in order to find the second peak in the Hough space which represents the opposite edge of the guide wire. Filtering out the Hough space in this manner is a necessary step because there is always the potential that there may be some noise in the image which is misconstrued for a line. In this way, once the first edge of the wire has been found, there is a much higher likelihood that the second peak found in the Hough space is actually a wire edge and not just noise. At this point in the image processing flow, the gross edge detection is complete. The results of the gross edge detection can be seen in Figure 17.



Figure 17 - The results of the Hough transform line detection on the left image show the wire edges outlined in green.

The next stage of the image processing is fine edge detection. The goal of this step is to locate the start and end of each black line that has been laser etched into the guide wire. To begin this stage, the image is cropped so that only the guide wire information remains in the image. The crop region is defined by the coordinates which outline the long edges of the wire; information gained in the previous image processing stage. Once the image is cropped it is then rotated so that the cropped wire is completely vertical. With the cropped wire image being vertical, the laser etched lines on the wire are now all in a horizontal orientation. A simple Prewitt horizontal edge filter can then be applied to the image so that the start and ends of the etched lines are now binary edges. The results of the horizontal edge filter can be seen in Figure 18.



Figure 18 - The results of the horizontal edge detection. The original image of the wire is shown on the left with the resulting edge image on the right.

With the horizontal edge image created, the next step is to detect the etched lines of the wire using another Hough transform. However, the Hough transform can only detect straight lines, not curved lines. As can be seen in Figure 18, some of the lines from the Prewitt filter appear curved. To correct for this and create an edge image suitable for line detection through the Hough transform, the initial horizontal edge image was stretched horizontally so that the curved lines in the image are straight. A Hough transform can then be applied to this stretched image to find each of the lines which define the start and end of the etched black lines on the wire. Once these lines are detected, they are converted into points which run along the center of

the edge image, which would also be the center of the wire. These points are then transformed back into the coordinate space of the original image. The results of this process for the left image can be seen in Figure 19.

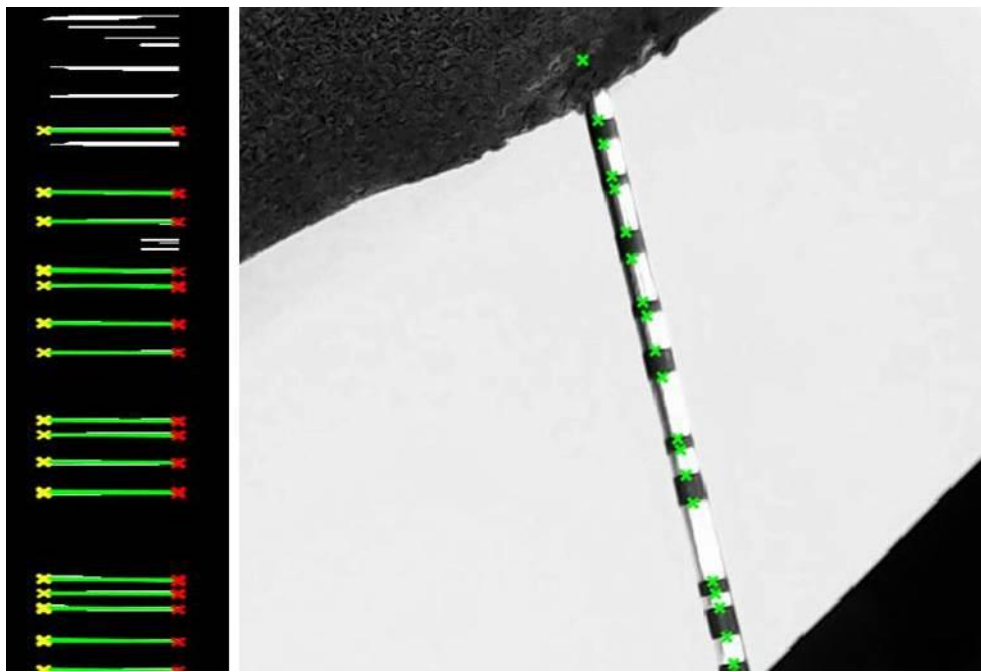


Figure 19 - On the left, the stretched horizontal edge image can be seen with lines labeled resulting from the Hough transform. On the right these lines can be seen mapped back on to the original image.

The feature points from both the left and right images are now used to reconstruct the 3D vector of the guide wire relative to the known location of the Sawbones femur. To do this, the Direct Linear Transform is once again used. The algorithm developed to reconstruct the wire vector begins by sorting both sets of feature points so that they are in order from closest to the bone to furthest from the bone. Subsets of the feature vectors are then randomly sampled, setting the sample size to be half the length of the smallest feature vector. These sampled feature vectors are assumed to perfectly correlate and are used to back project their points in 3D space. The

equation used to calculate this back projection is a reorganization of equations 1 through 4, which defined the relationship between the L and R image parameters, the U and V coordinates of the 2D images, and the X, Y, and Z coordinates of the calibration object. In this reorganization, the L and R parameters and the U and V image coordinates are all known values. The only remaining unknowns are the X, Y, and Z coordinates of the guide wire vector. This equation can be seen in Figure 20.

$$\begin{bmatrix} L_1 - L_9u_L & L_2 - L_{10}u_L & L_3 - L_{11}u_L \\ L_5 - L_9v_L & L_6 - L_{10}v_L & L_7 - L_{11}v_L \\ R_1 - R_9u_R & R_2 - R_{10}u_R & R_3 - R_{11}u_R \\ R_5 - R_9v_R & R_6 - R_{10}v_R & R_7 - R_{11}v_R \end{bmatrix} \begin{bmatrix} x \\ y \\ z \end{bmatrix} = \begin{bmatrix} u_L - L_4 \\ v_L - L_8 \\ u_R - R_4 \\ v_R - R_8 \end{bmatrix}.$$

Figure 20 - This system of equations allows the X, Y, and Z coordinates of the wire vector to be back projected [68]. The system is again solved using a Moore-Penrose pseudo-inverse method.

After solving for the 3D coordinates of the guide wire from the initial subset of feature points, the quality of the reconstruction is evaluated. The 3D points that make up the wire are fit to a line using a built in Matlab function. If the points were correctly reconstructed, than the resulting correlation coefficient from fitting the line will be close to 1. If the coefficient has a low value, then the subset of feature points used to reconstruct the wire was not correctly chosen and a new subset of feature points must be chosen. This process of selecting a subset of points, reconstructing their 3D vector, and evaluating that vector continues to proceed until a threshold correlation value has been met (.999). For the interest of creating the virtual radiograph in a timely manner, if the number of iterations for this process exceeds 100 before the threshold has been achieved, than the best reconstruction is chosen as the 3D vector of the guide wire. In either

case, this step outputs the guide wire's vector in space relative to bone. The only remaining degree of freedom to define is where the tip of the wire sits along this vector.

The address assessment stage uses a normalized cross correlation (NCC) algorithm to determine the position of the wire tip within bone. The algorithm operates by taking the cropped section of wire generated in previous image processing steps and comparing it to a template of the complete wire address scheme. The comparison is quantified by calculating the sum of squared differences between the image and the section of the template being compared to. This value is then divided the standard deviation of both the image and template [73]. The equation for this calculation can be seen below. In this equation,  $A_{uv}$  is a pixel value in the wire image,  $B_{uv}$  is a pixel value in the template,  $\bar{A}$  is the mean of the pixel intensities in the wire image, and  $\bar{B}$  is the mean of the template intensity values for the region that is being compared.

$$r = \frac{\sum_u \sum_v (A_{uv} - \bar{A})(B_{uv} - \bar{B})}{\sqrt{(\sum_u \sum_v (A_{uv} - \bar{A})^2)(\sum_u \sum_v (B_{uv} - \bar{B})^2)}} \quad (8)$$

Due to the varying positions that the wire can be placed relative to each camera when the simulator is in use, the scale of the wire template that best matches the cropped image of wire can change. In order to optimize the agreement between the wire image and the wire template, the normalized cross correlation is iteratively calculated as the size of the template is incrementally adjusted. The template is scaled in size from its initial size to three times its initial size, in increments of 10%. Correlation values are calculated at each incremental scaling of the template. The maximum correlation that is found is taken as the best match between the wire image and template image.

When a maximum correlation is found between the cropped wire image and the template, the position along the template where the maximum correlation was found represents the offset of the wire tip relative to the imaged section of wire. This piece of information coupled with the wire vector relative to bone that was previously calculated allows the virtual image to be generated. A virtual STL file of a guide wire that has been placed in the same coordinate system of the laser scanned femur is taken from its initial position and rotated and translated to be aligned with the vector of the wire outside the bone. From there, the wire is translated toward the bone by the offset calculated during the normalized cross correlation calculation. It is at this point that the virtual image is presented to the resident. An example of a virtual image can be seen in Figure 21.

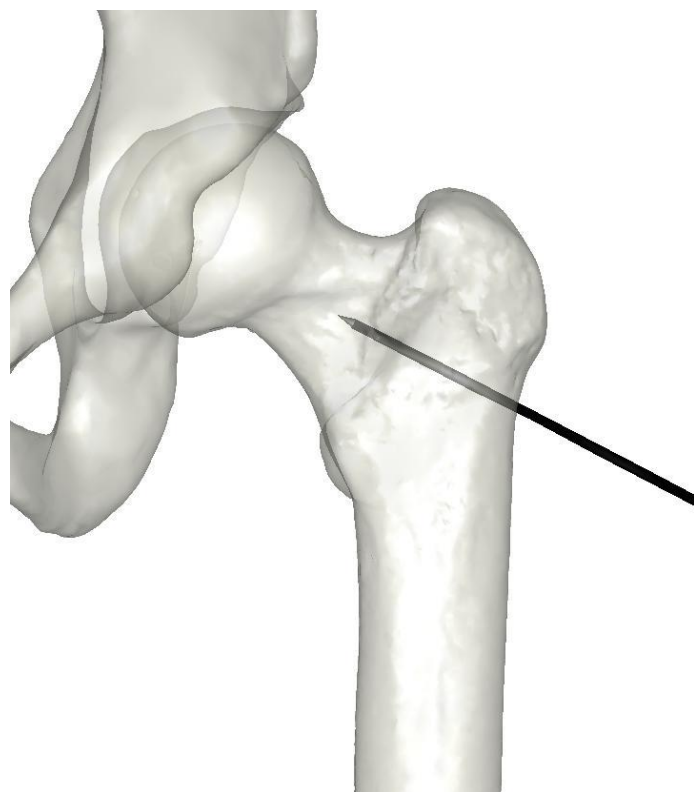


Figure 21 - An example of a virtual AP radiograph that could be presented to a resident.

### Design Iteration 1 Issues:

Initial laboratory testing of the simulator was performed to assess the accuracy in locating the wire relative to the Sawbones femur. These tests were performed by placing the tip of the wire on different calibration points and comparing the calculated coordinates of the tip with the known coordinates of the calibration point. Four calibration points were measured which resulted in an average accuracy of 2.27mm.

Although initial laboratory testing suggested that the accuracy of the simulator was acceptable for training purposes, field testing showed that the overall design was not very reliable and was prone to large errors which completely misrepresented where the wire was actually being placed in bone. When training with residents, the guide wire could often be projected as being drilled deep into the bone when the resident was actually just beginning to assess his or her wire trajectory outside of bone. At times the wire trajectory could be displayed in a virtual image as being angled severely to the anterior side or even out of bone when it was obvious that this was not the case. Additionally, at times the simulator would take an unacceptable length of time to calculate the virtual image, sometimes longer than 5 or 6 seconds. With these issues present during field testing it was clear that there were several major flaws in the initial design of the simulator and that the design needed to be changed in order to have a successful and reliable simulator available for resident training.

## Design Iteration 2:

### Hardware Design:

The second iteration of the simulator can be seen below in Figure 22. Although I will present all components of the second simulator design, it is important to note the Dr. Geb Thomas contributed a significant amount of the work that went into redesigning the hardware of the simulator. At the conclusion of discussing the design of the second iteration a table will be presented which highlights the components that Dr. Thomas designed individually, the components which I designed individually, and the components which were designed in a collaborative manner.

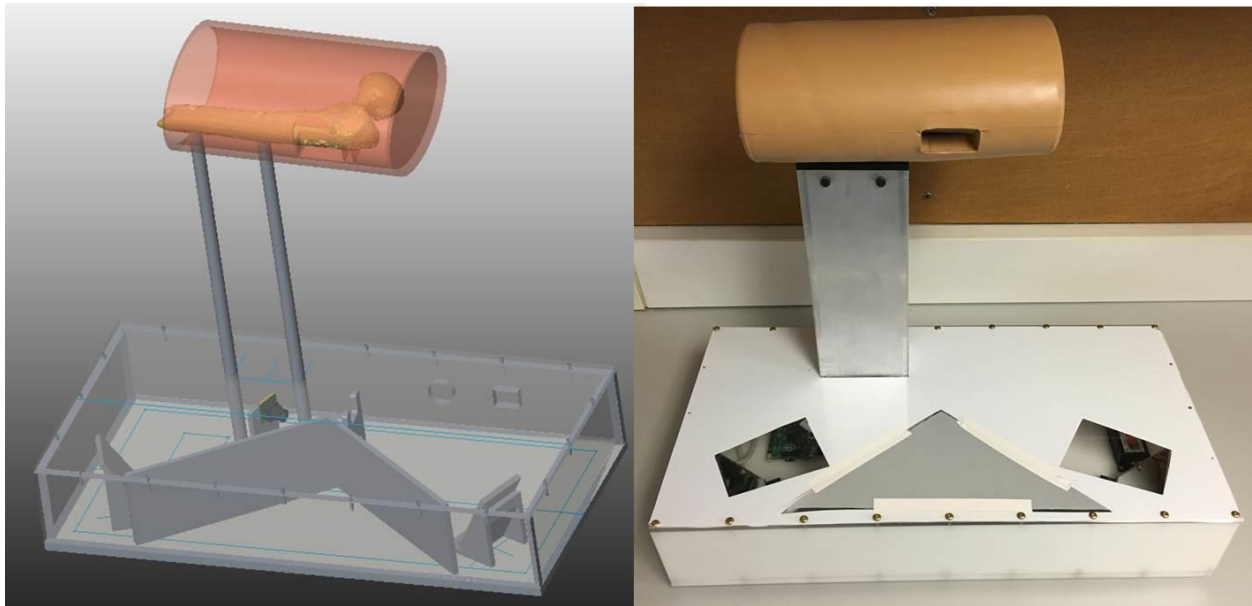


Figure 22 - On the left is a rendering of the simulator in Creo. On the right is an image of the physical simulator. The LED lights are not visible in either image.

The hardware design of the second iteration varies in many ways from the initial design of the simulator. In this design, one camera attached to a Raspberry Pi machine (model 2 B+)

acquires images of the scene. The single camera image is split by an initial mirror so that half of the rays leaving the camera are diverted and half remain in a straight line. These two separate image paths both intersect with mirrors which are angled upward toward an area where the guide wire is intended to be placed. In this way, two orthogonal images of the guide wire workspace can be captured with a single image from one camera.

In this design iteration, the proximal femur is mounted to two rigid posts at a height of 13 inches from the base of the simulator. The femur was mounted at this height to provide ample space for a resident to move and maneuver the guide wire drill without being impeded by the physical surface of the simulator. The femur is again mounted with a 15° angle of anteversion. The soft tissue envelop is a customized sleeve developed with Sawbones to provide a more realistic look and feel of soft tissue, similar to many of their other products. In designing the sleeve, a two inch wide by one inch tall window was included to act as an incision made by a surgeon that is being kept open with surgical instruments. This window was designed to be located so that it is roughly centered on the lesser trochanter of the proximal femur, a common entry point for a guide wire in this procedure.

Three LED light strips are mounted to the base of the simulator facing up towards the insertion area of the guide wire. Similar to the first design, these lights are intended to flood the area imaged by the camera with light to both provide adequate visibility of the guide wire, and to reduce the effect of room lighting on the image processing algorithms. Because these lights are pointed upwards towards the face of someone using the simulator, a sheet of diffuse plastic material is mounted to the clear Plexiglas surface of this simulator. This allows the light to pass through and provide adequate illumination of the guide wire without producing a glaring light source directed at a resident/user.

A separate calibration object was designed for this simulator. The calibration object was designed so that the calibration points would span the region that the guide wire was intended to be placed. Given the complex geometry of this calibration object, the target was 3D printed on a Fortus 250mc 3D printer. This printer can print in multiple colors and in layers as thin as 0.17mm [74]. To place the calibration object in the same coordinate frame as the proximal femur, both the proximal femur and calibration object were laser scanned and aligned using Geomagic software. Similar to the first design iteration, the 3D coordinates of the calibration object relative to the femur were then queried in Geomagic and recorded for later use when calibrating the camera to the scene of the simulator. The laser scan of the calibration object and proximal femur can be seen in Figure 23.

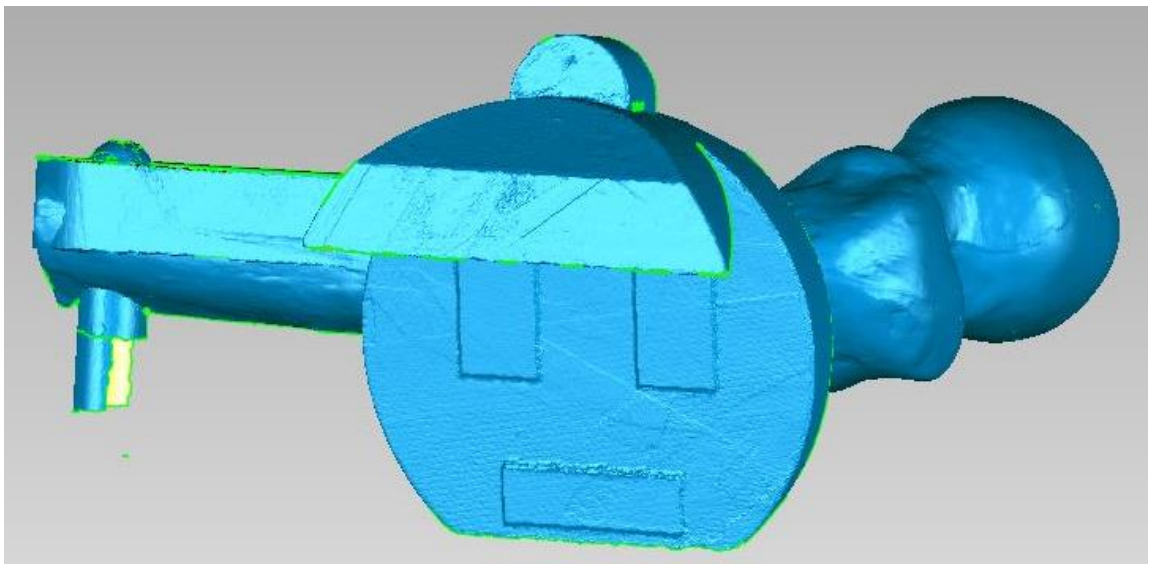


Figure 23 - The calibration object and proximal femur can be seen registered in Geomagic. Additional calibration points on the top surface of the calibration object are not visible from this view.

A new laser etch address pattern was also developed for the second iteration of the simulator. In the first addressing scheme, similar looking wire addresses were often confused for

one another in the normalized cross correlation step of the image processing. In order to prevent this from continuing to happen, a new pattern was designed so that each address was unique and would not be confused with neighboring addresses. This addressing scheme was based on the idea that every address should contain binary units that are either “on” or “off” and that “on” units should never repeat back to back. The addresses start out with  $2^0$  combinations of binary units, then  $2^1$  combinations, then  $2^2$  combinations, and so on. Between each binary address is a start/stop node. Binary unit spaces were given a length of L, where L is set to .5mm, and the start/stop nodes given a length of 2L. This pattern was also extended to run further along the guide wire than the original etching pattern. Field testing showed that near the very end of placing a guide wire, almost no address was visible to the cameras. In order to ensure that several addresses are visible to the cameras when the tip of the wire is near the apex of the femoral head the binary pattern was extended for 200 mm, 65 mm longer than the first laser etched pattern. An image of this new binary addressing scheme can be seen below. For additional information on details of the pattern, see Appendix 1.



Figure 24 - The new wire etched pattern is shown here.

These components make up the hardware that was designed for the second iteration of the simulator. The table below highlights design contributions that were made solely by Dr. Thomas and those that were made in a collaborative effort.

Table 1 - Hardware Design Contributions

Design Feature	Dr. Geb Thomas	Collaboration
Camera Position		
Mirror Angles		
LED lighting		
Calibration Object		
Soft Tissue Envelope		
Wire Etch Pattern		

#### Software Development:

In the second iteration of simulator development, some of the image processing techniques have carried over and some have changed. Of the techniques that have carried over, there are most likely minor tweaks that have been made to correct for bugs written into the software. However, in an effort to highlight the major and more important changes that have been made, these minor tweaks will not be mentioned. Instead, the main image processing steps that carry over between designs will simply be acknowledged.

The first major new step in the software is in acquiring images from the Raspberry Pi camera. Because the Raspberry Pi is essentially a computer of its own, a method of communicating between the laptop, which runs the Matlab image processing code, and the

Raspberry Pi, which controls the camera, needed to be developed. To establish this communication, two Python scripts were written; one saved to a directory on the laptop and one saved onto the Raspberry Pi. These scripts establish a socket communication between the Ethernet port on the Raspberry Pi and the Ethernet port on the laptop. The Raspberry Pi is established as the main server and the laptop is established as the client accessing the server. When the Python script is run on the laptop, it begins by attempting to connect with the static I.P. address of the Raspberry Pi machine. Once this connection has been established, the Raspberry Pi camera turns on and begins acquiring images in a continuous nature. These images are continuously sent through the socket connection and into a directory established on the laptop. In this directory, every time a new image is received, it writes over the previous image. With this protocol intact, when a resident requests a virtual image, the Matlab code begins by pulling the most recently transferred image from the directory of the laptop. This image is then split into two images that represent the camera rays from the orthogonally positioned mirrors facing the workspace of the resident.

For the most part, the first step in the image processing sequence remains largely the same. A difference image is used to isolate the wire in the image. This difference image is then taken through a Canny edge detection and a Hough transform to find the outline of the wire in the image. One main addition to this step however is that a mask is applied to the difference image before the Canny edge detection and Hough transform are applied. This mask has been designed in both images to discard regions of the image that the wire could never be placed and retain only regions where it is likely that the wire will be in the image. In this way, the chance of finding the wire in the image and not random noise increases from the first iteration of the

software development. An image of the output from this first step in the new simulator can be seen in Figure 25.

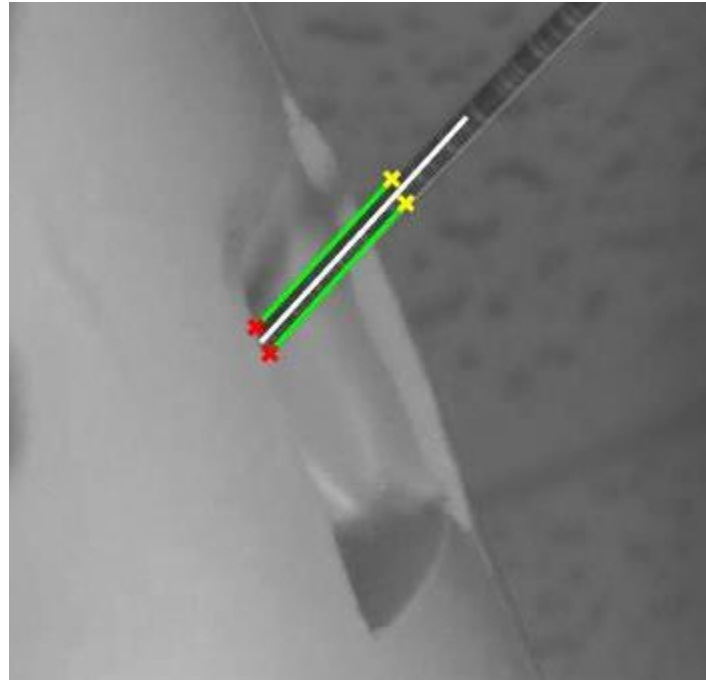


Figure 25 - The outline of the wire is found in the left image of the new simulator.

The image is then cropped and rotated as it was in the previous software iteration. However, an additional step has been added to enhance the contrast of the cropped region of wire. In this step, an adaptive histogram equalization algorithm is applied to the cropped image. This algorithm works by taking small regions of the image and calculating a histogram equalization mapping for that region. The mapping is then applied to the central pixel in the region and this process is done for all pixels in the cropped image [75]. This step results in an image where regions of contrast have been enhanced and homogenous regions have been left relatively unchanged. This helps to reduce the effect of bright or dark patches that may appear on the guide wire in capturing an image. The results of applying this algorithm can be seen in Figure 26.

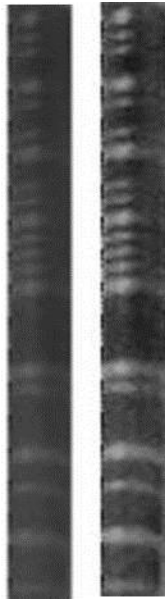


Figure 26 - On the left is the cropped region of wire before adaptive histogram equalization is applied. On the right is the cropped wire after adaptive histogram equalization is applied.

Once the left and right images have both been cropped and enhanced, each image is run through the pattern matching algorithm previously described. In the initial development of the simulator, only one image was required to run through the pattern matching algorithm. However, in the new implementation, this algorithm now serves two purposes; to calculate the offset of the wire tip from the imaged region of wire, and to generate a binary image that can be used to extract the feature points of the etched wire lines in each image. When the normalized cross correlation identifies the region of the template that best matches the cropped image, that region is saved and scaled to match the exact size of the cropped wire image. Given that this image is a perfect binary image, the transition between white and black regions now identifies where etched lines are and the cropped images no longer have to go through the Prewitt horizontal edge filter and Hough transform. The cropped images and their corresponding binary images can be seen in Figure 27.

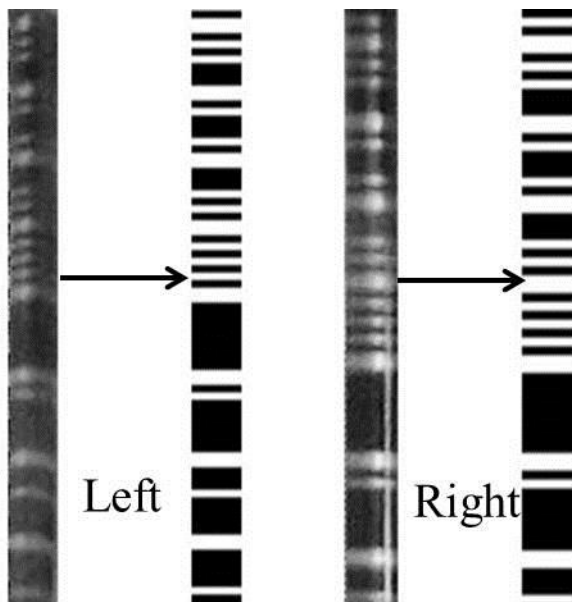


Figure 27 - The resulting binary images from the templating matching algorithm.

Unfortunately, the pattern matching algorithm may not always correctly identify the region of the template which matches the cropped image. To check for this, after both the left and right images go through pattern matching, the difference between the wire offset values for each image is calculated. If the difference between these offset values is more than 20 mm, it is likely that one of the templates has been incorrectly matched. In this case, the cropped image with the highest correlation to the template pattern is assumed to be the correct match case. The opposite image is then run through an additional pattern matching step, this time only examining the region of the template which falls within the region correctly found in the other image. For instance if the left image was correctly found to be offset from the wire tip by 50 mm, then the right image would only include the region of the template that extends just before this and just beyond this point in its pattern matching search. In this way, the pattern matching step is much more likely to find the region of the template which correctly matches the cropped wire.

Once the template matching has been completed and verified for both images, the binary images are then used to extract the start and end points of each etched line on the guide wire. When these points have been identified on the binary image, they are then transformed back into the original image coordinates of the image captured by the Raspberry Pi cameras. The result of this feature extraction can be seen below in Figure 28.

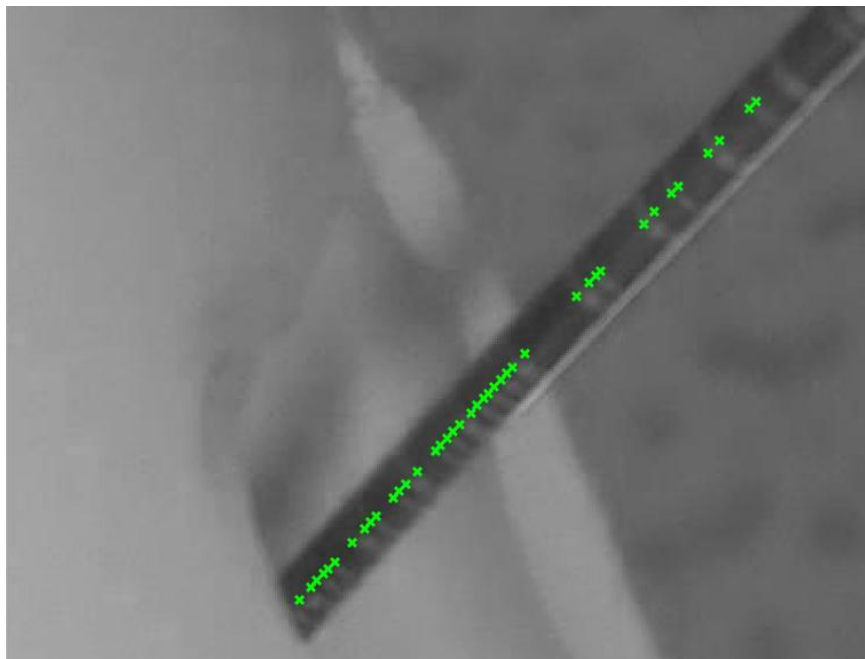


Figure 28 - The start and stop of each etched black line can be seen here for the left image. Similar results are produced in the right image.

With the feature points extracted from both the left and right images, the 3D vector of the wire is once again calculated using the Direct Linear Transform algorithm. However, given that the pattern matching algorithm was run on both the left and right images prior to running this step, more apriori information can be used to guide the calculation of the 3D vector reconstruction. Given that the offset of the wire tip is known for both images, we can immediately disregard any points that would appear in one image but not the other. For instance,

if the left wire tip is offset by 45mm and the right wire tip is offset is 35mm, then the feature points on the right image which make up the 10mm difference in offset should be disregarded, because in the left image, those points are not visible or were not detected. With this adjusted list of feature points, subsets of the points can iteratively be used to reconstruct the 3D vector of the guide wire. As was previously discussed, the calculated wire vector will be selected if it either meets a threshold value for linear correlation, or it has the maximum correlation value after running through all potential iterations of corresponding feature points.

With the DLT reconstruction algorithm complete and the wire offset known from the pattern matching stage, the virtual radiograph can once again be created. This final step concludes the image processing development for the second design iteration.

## **Chapter 3: Simulator Assessment**

### Simulator Accuracy:

In order to ensure that residents using the surgical simulator are being shown correctly depicted virtual radiographs, the accuracy of the simulator was studied. To properly assess the accuracy of generating a virtual radiograph, the wire must be placed at a known location in bone with a known trajectory. To create a series of known wire locations, two target sawbones were created as can be seen in Figure 29. These sawbones were drilled with holes in locations and trajectories that spanned the guide wire window provided on the soft tissue sleeve. The drilled holes were then filled with a copper tube whose inner diameter is just slightly larger than the diameter of the guide wire used with the simulator. The ends of the copper tubes were filled with a metal stopper and the tubing was cemented in bone. This created a reproducible slot that the guide wire could be placed in while also being held securely in place. The metal stopper at the end of the copper tubing ensures that the wire would be placed at the same depth each time it was inserted into a copper slot.

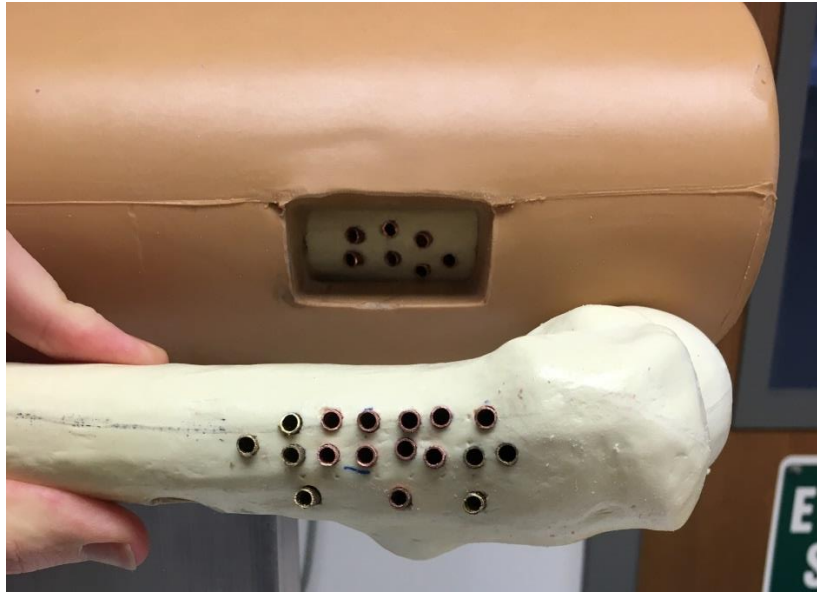


Figure 29 - The target sawbones are pictured here. The target slots are shown to cover the workspace provided in the window of the soft tissue envelope.

To relate the locations of the slots drilled into the bone with the coordinate space of the sawbones femur, a laser scan of the setup was obtained. In this process, a wire was placed inside one of the copper slots and then laser scanned with the FaroArm laser scanner. A shorter wire than the normal guide wire was used in this process so that the end of the wire could easily be captured during the laser scan. After one laser scan of the wire was complete, the wire was removed from the slot and placed into a new slot for laser scanning. This was repeated for each copper slot cemented into the sawbones.

Once the laser scans were obtained, the models were aligned in Geomagic to previously obtained scans of the sawbones femur. This alignment placed the laser scanned wire slots in the same coordinate space used to reconstruct the wire vectors and generate the virtual radiographs. The trajectories of each laser scanned wire were automatically known based on the point cloud which defined each wire. The depth of the wire in bone was then defined by starting at the end

point of each wire captured during laser scanning and projecting the known length of the scanned wire along the known trajectory of each wire. Thus, each copper slot has a known wire trajectory relative to bone and a known wire tip location relative to bone. An image of the aligned laser scanned wires in one of the sawbones can be seen in Figure 30.

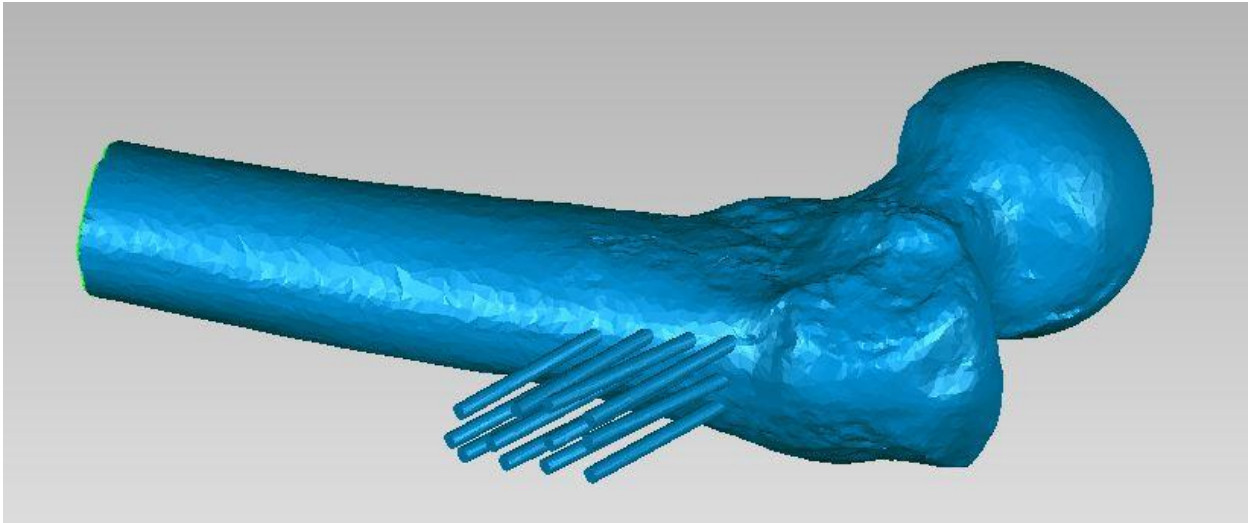


Figure 30 - One of the laser scans of the copper slotted sawbones can be seen here. The wires have all been aligned and projected into the coordinate space of the sawbones femur.

The accuracy of the simulator can then be measured in a very simple manner. The guide wire can be placed in one of the copper slots in a sawbones femur and imaged as if the simulator were being used by a resident. The simulator then calculates the measured position and trajectory of the guide wire in this location. The accuracy of the simulator at the location is calculated as the difference in degrees between the trajectory of the known wire position and the measured wire position, and the Euclidean distance between the measured tip of the guide wire and the known location of the tip. This accuracy measurement was performed at each copper slot in both sawbones. Additionally, the accuracy at each slot position was measured ten times to assess both the consistency of the simulator and ensure that a valid measurement was taken.

Because different lighting conditions and testing locations played a large role in the performance of the first design iteration, the accuracy of the simulator was also measured across a variety of locations. The initial accuracy of the simulator was measured in an ideal laboratory setting to assess what the performance of the simulator could be under ideal conditions. The simulator was then taken to additional locations where the simulator could reasonably be expected to be used by a residency program for training purposes. These tests were performed not necessarily to examine how accurate the simulator was, but were instead aimed at examining how the performance of the simulator changed across varying lighting and room conditions.

#### Accuracy Results:

The simulator accuracy was measured under ideal conditions through a total of 290 wire reconstructions (29 different copper slots, 10 readings per slot). In these readings, the wire tip accuracy varied between .25mm and 4.85mm of error. On average the wire tip error was 1.43mm. The average standard deviation between repeated measurements was .44mm, suggesting that the calculated wire tip positon may change on average less than half of a millimeter if a new reconstruction is performed but the wire position does not change. The wire angle error was also measured across the 290 measurements. In these readings, the wire angle error varied between  $.04^\circ$  and  $4.3^\circ$ . The average angle error was  $.93^\circ$  and the average. A figure illustrating how these errors varied by the guide wire position relative to the femur can be seen in Figure 31.

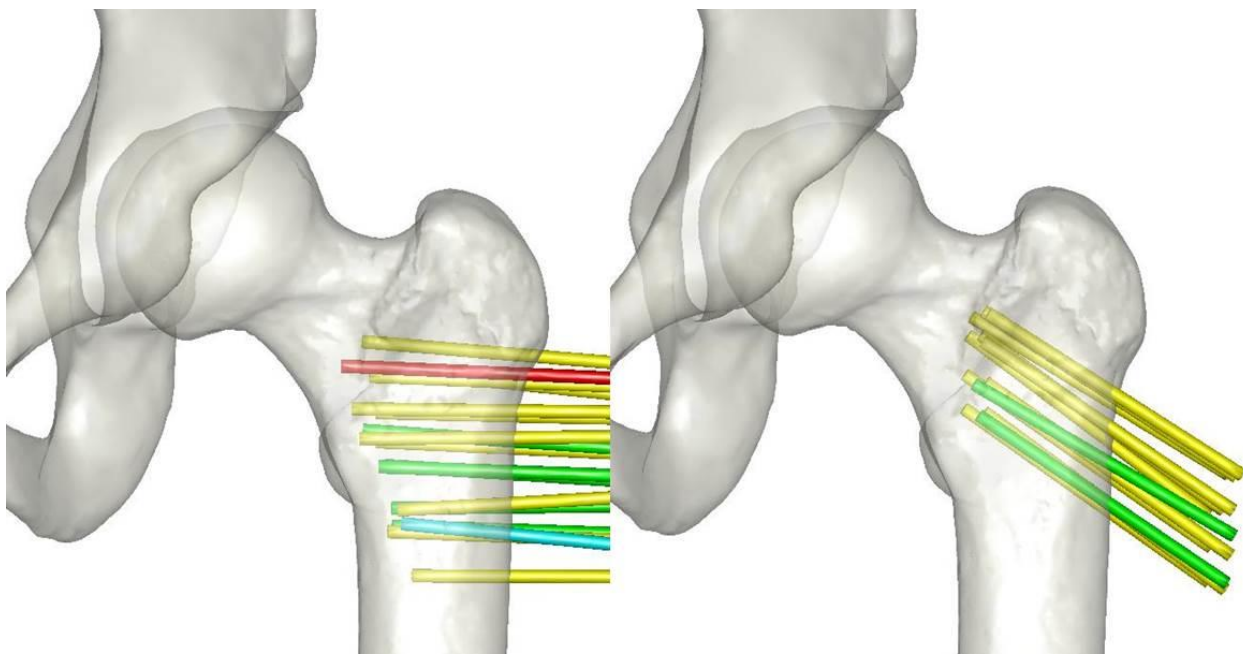


Figure 31 - The wire error based on guide wire position is shown here. Wires colored in green have less than 1mm of error on average. Yellow wires have errors ranging between 1 and 2mm. Blue wires have errors ranging between 2 and 3mm. Red wires have an average error greater than 3mm.

When testing across multiple locations, only the second target femur was used. In this testing, the average tip error did not vary greatly in changing locations. The greatest amount of change observed was a difference of .44mm between the first and fourth testing locations. Overall the average tip error was 1.7mm and the average angle error was 1.2 degrees, both similar values to the testing results done under ideal conditions. The time to compute the wire position was also recorded during this series of tests. The average length of time across the different testing locations was 1.05 seconds. A summary of these results can be seen below in Table 2.

Table 2 - Wire Accuracy Results Across Multiple Locations

<b>Location</b>	<b>Average Tip Error (mm)</b>	<b>Average Angle Error (degrees)</b>	<b>Average Computation Time (seconds)</b>
Desktop, No Room Lighting	1.53	1.15	1.12
Biomechanics Dry Lab	1.59	1.31	1.03
Biomechanics Conference Room	1.61	1.12	1.01
Ortho Skills Lab	1.97	1.18	1.08
Ortho Library	1.81	1.31	.99
<b>Average:</b>	<b>1.7</b>	<b>1.2</b>	<b>1.05</b>

Discussion:

These results illustrate that the current simulator design provides both reliable and accurate virtual radiograph images. When considering that the target area for placing the guide wire in the femoral head is a 25mm region, projecting the guide wire tip within roughly 1.5mm of its true location and within a degree of its true trajectory should provide a more than sufficient representation for the purposes of training and skill development. Furthermore, these results compare well to other simulators published in the literature. In their work developing a hip wire navigation simulator, Thomas et al. showed that the simulator had an average accuracy of 3.57mm when locating the wire tip [62]. Additionally, the virtual radiographs are shown to users in roughly one second. This will appeal to residents who may be used to seeing radiographs appear within the same time frame when using a C-arm during a normal surgery.

## **Chapter 4: Simulator Implementation**

### Training with Residents:

Once the simulator design and laboratory testing were complete, the simulator was implemented as part of a surgical skills training day at the University of Iowa. Six first year residents participated in the study. The training day began by introducing the residents to the task of hip wire navigation through a didactic lecture given by an attending physician. After the procedure had been explained, each resident proceeded to attempt the wire navigation task in a pseudo operating room environment. In this setup, a Sawbones femur is placed inside a soft tissue envelope that has been molded to look like a left human leg. The Sawbones femur is coated with a radio-opaque dye, making it visible when imaged with fluoroscopy. AP and lateral images of the femur were provided to the resident through a C-arm fluoroscopic unit. The residents were instructed to place a guide wire in the Sawbones femur so that the tip apex distance (TAD), or the distance between the guide wire tip and the apex of the femoral head, was minimized. Residents were also told to balance minimizing the TAD with the number of radiographic images that were acquired and the total amount of time the procedure took. Because of the potentially harmful effects of receiving ionizing radiation it is important that residents learn to be judicious in their use of intra-operative imaging. This initial exercise provided a baseline skill level assessment of the residents on the task of hip guide wire navigation.

After the baseline assessment with the C-arm was completed, the residents were split into two groups. Group 1 followed the C-arm exercise with a 30 minute training session using the simulator, followed by two more post-simulator assessments using the C-arm. On the other hand, Group 2 followed the initial baseline assessment with another C-arm exercise, followed by a thirty minute training session on the simulator, and then one final assessment using the C-arm.

This type of experimental design is commonly referred to as a cross-over design. The cross-over experiment style is designed to distinguish between improvements on the task that might come from repetition alone and improvements that come from the intervention of training with the simulator. In this paradigm, slight improvements might be made between successive repetitions of the C-arm exercise, but significant changes in skill level and behavior are more likely to be observed after the training session with the simulator. A diagram laying out the cross-over schedule can be seen in Figure 32.

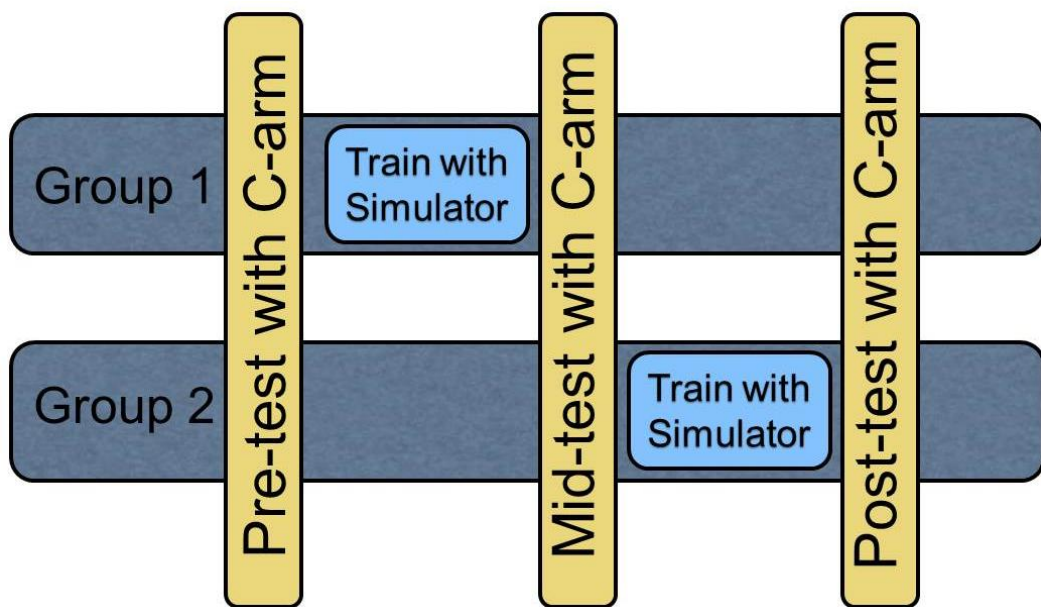


Figure 32 - The schedule used to train the resident is shown here.

In the training session with the simulator each resident went through at least four iterations of practicing to place the guide wire. When working with the simulator, two levels of training were presented, a beginner level and a more advanced level. The beginner level was designed to provide residents with feedback that would help with their ability to place the guide wire in bone. Feedback was provided to the residents in several forms. First, a target area was overlaid on the virtual radiographs of the proximal femur in both the AP and lateral images. This

target area was intended to provide residents with a visual guide of potential trajectories of the guide wire which would result in a clinically acceptable tip apex distance. The resident could compare the trajectory of their placement of the guide wire with these target paths and adjust as needed. In addition to the target paths, messages with instructions on how to adjust one's hand position and wire angle were displayed to the resident in the interface of the simulator. For instance, if the guide wire was angled to far posteriorly in the lateral view relative to the femur, the message would indicate that the wire trajectory should be angled in a more posterior direction and that the resident needed to drop their hand to achieve this wire trajectory. These messages were intended to provide direction and feedback to the resident as if they were working with an advising physician.

Residents practicing in the first level of the simulator were also provided with information about the quantitative measure of their performance each time a virtual radiograph was requested. The simulator interface displayed the total amount of time that the procedure was taking, the number of AP and lateral images that the resident had requested, the current tip apex distance of the guide wire, and a cumulative score that combined these metrics. The cumulative score was calculated based on the equation shown below. Residents were not explicitly told how this cumulative score was calculated, however they were told that it was a combination of the length of duration of the procedure, the number of images requested, and the tip apex distance, with an emphasis on the TAD. Residents were instructed that better performance equated with a lower score on the simulator.

$$\text{Score} = \text{Number of Seconds} + \text{Number of Images} + 10 * \text{TAD} \quad (9)$$

An example of the beginner level interface can be seen in Figure 33. The level 2 version of the simulator was designed to be more representative of the feedback that was given when working with the C-arm exercise or in the operating room. In this level, only the AP and lateral virtual radiographs were shown to residents. There were no target trajectory paths overlaid on the images or information provided about the guide wire's tip apex distance. When training with the simulator the first three sessions were done practicing on the beginner level of the simulator so that the resident could use the feedback to alter their technique and improve their skill. The fourth session with the simulator was performed using the second level of the simulator. This allowed the resident to practice transitioning back to an environment more similar to the C-arm before they actually returned to the C-arm exercise.

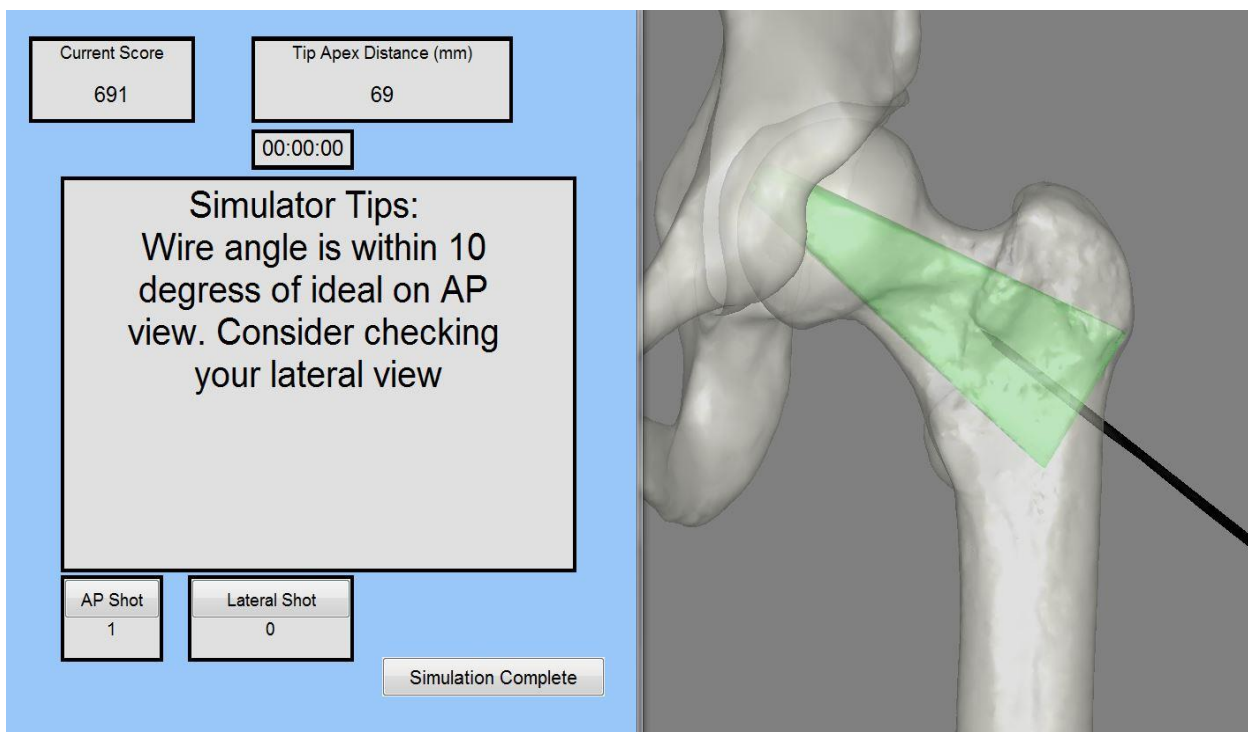


Figure 33 - The level 1 interface is shown here. On the right, an AP radiograph is shown. The green path in the virtual image provides a target path for the resident when placing the guide wire. Simulator tips and quantitative metrics of performance are displayed on the left half of the screen.

### Training Results:

Results from training with residents can be broken down into two main categories; performance on the C-arm exercise and performance with the simulator. These two categories are certainly related to one another; however they represent different forms of skill assessment. For instance, improvement on the simulator may illustrate skill development and learning, whereas improvement in the C-arm environment illustrates transfer of skill between the simulator and the pseudo OR.

The average score of each resident over the course of the four trials with the simulator is shown in Figure 34. The scores on the simulator show a negative slope across the four trials, with a high correlation value of .63. When the cumulative score is broken down by its components, similar trends can be seen in the duration of the procedure and the number of images used, but not for the tip apex distance. These results can be seen in Figure 35, Figure 36, and Figure 37.

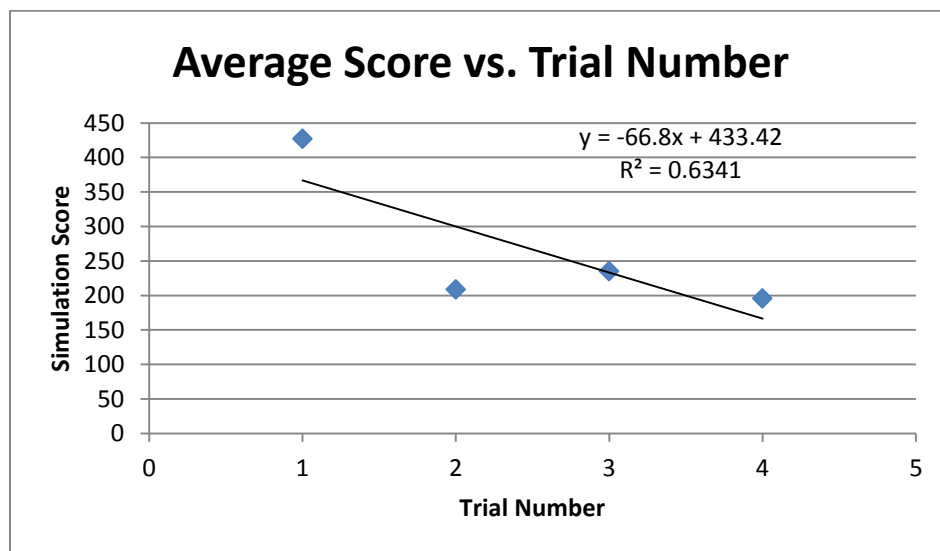


Figure 34 - The average simulator score across four trials is shown here. A negative trend in score, or improvement, is clearly visible in this chart.

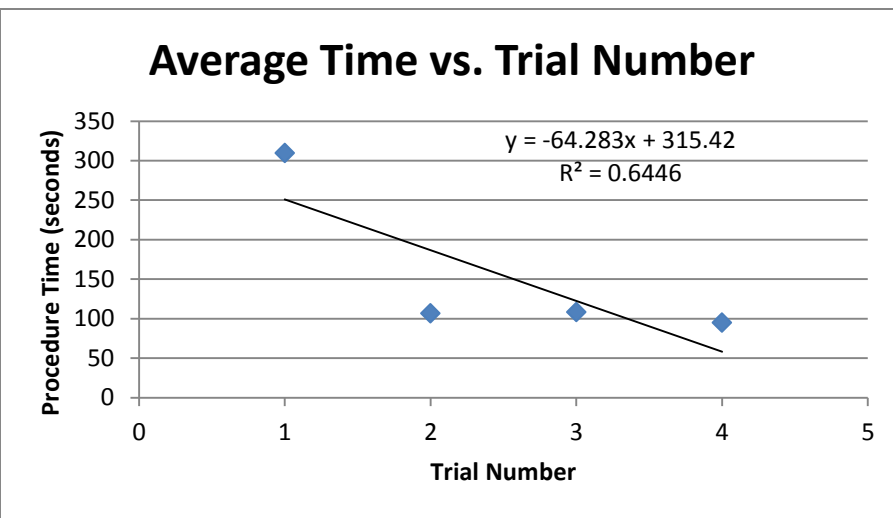


Figure 35 - The average procedure time across four trials is shown here.

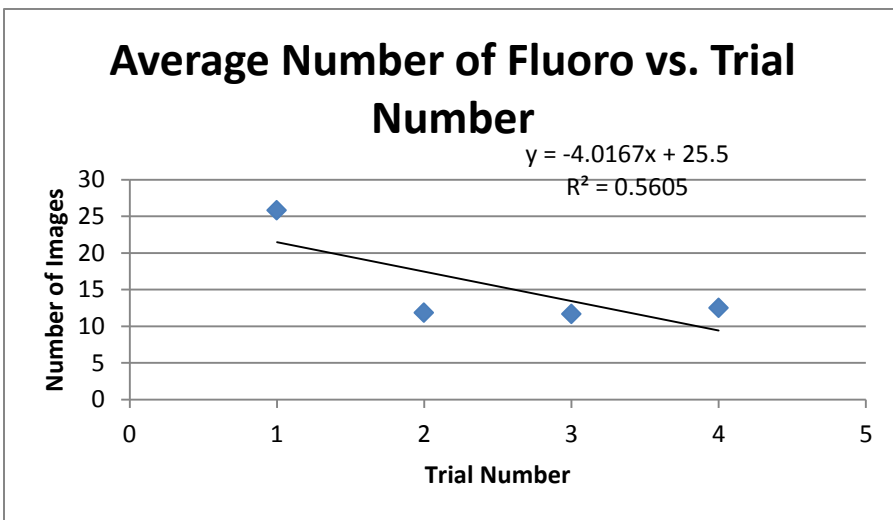


Figure 36 - The average number of fluoro images used across four trials is shown here.

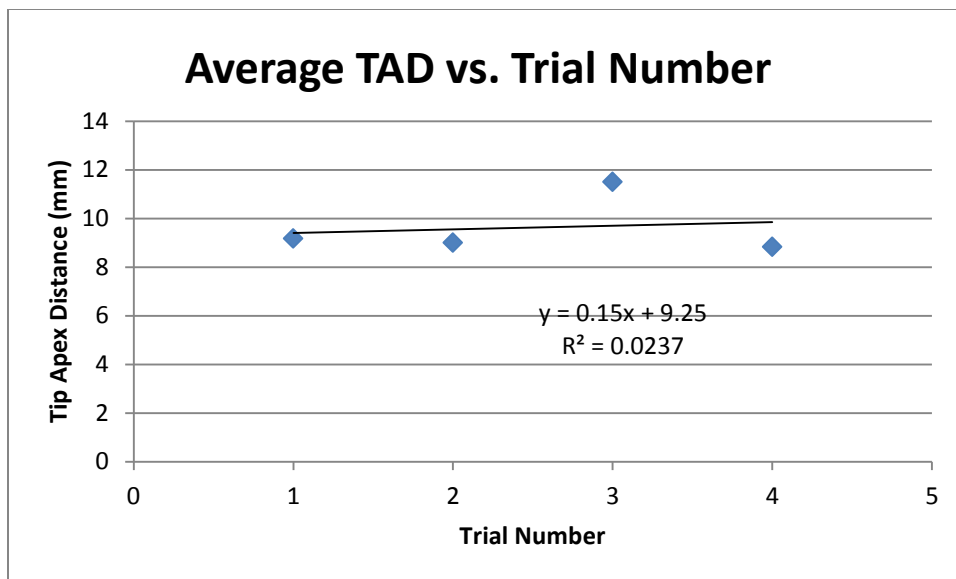


Figure 37 - The average tip apex distance across four trials is shown here.

The radiographic images taken during the C-arm exercise were also saved for each resident so that they could later be used to calculate the same score that was provided while practicing with the simulator. Having the same score on both of the training exercises allows performance on the simulator to be directly compared with performance on the C-arm exercise. The scores for the resident's performance on the C-arm exercise across all three trials can be seen in Figure 38. The results are separated by the group that each resident was in to observe the impact that training on the simulator had. To protect the identities of the residents, codenames were given to each participant.

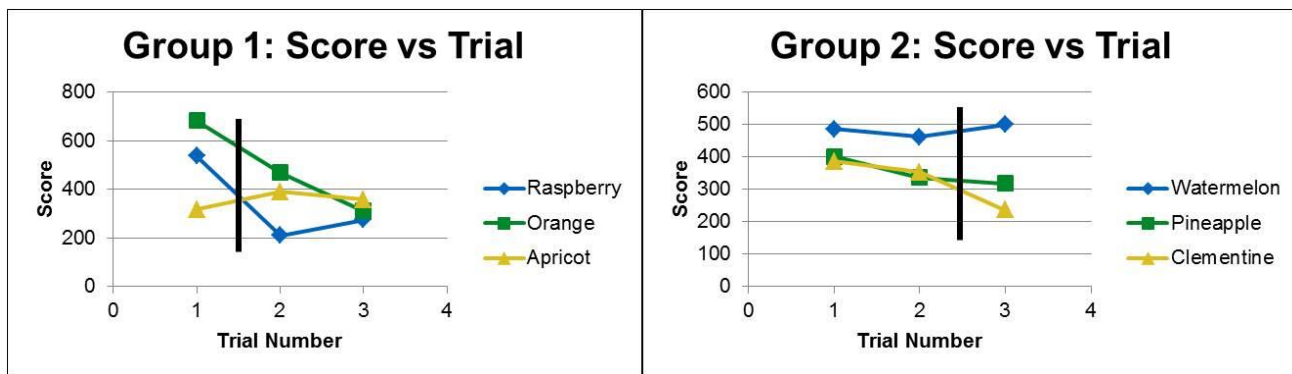


Figure 38 - Group 1 and Group 2 C-arm exercise scores are shown here. The black line indicates that practicing with the simulator occurred between the trial numbers.

A breakdown of the scores achieved on the C-arm exercise into their components can be seen in Figure 39, Figure 40, and Figure 41. Similar to the results seen in training with the simulator, a decrease in the procedure duration and number of radiographic images used can be observed across C-arm exercises.

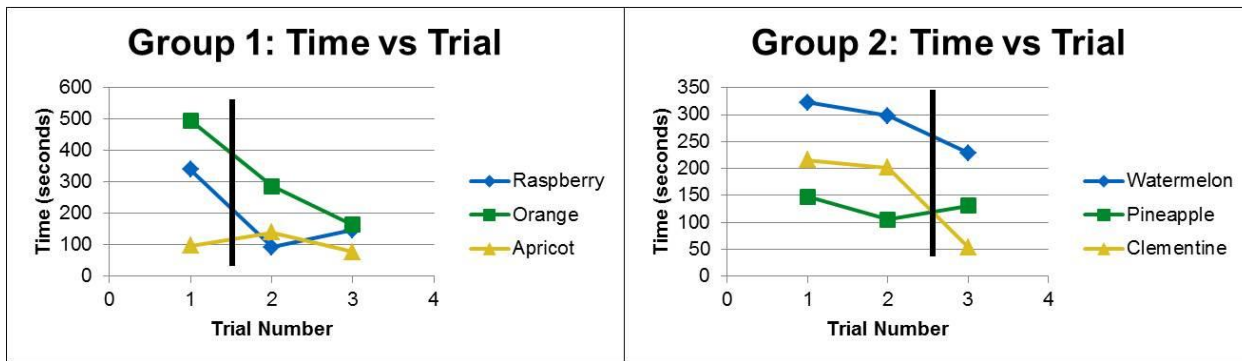


Figure 39 - Group 1 and Group 2 C-arm procedure duration over three sessions is shown here.

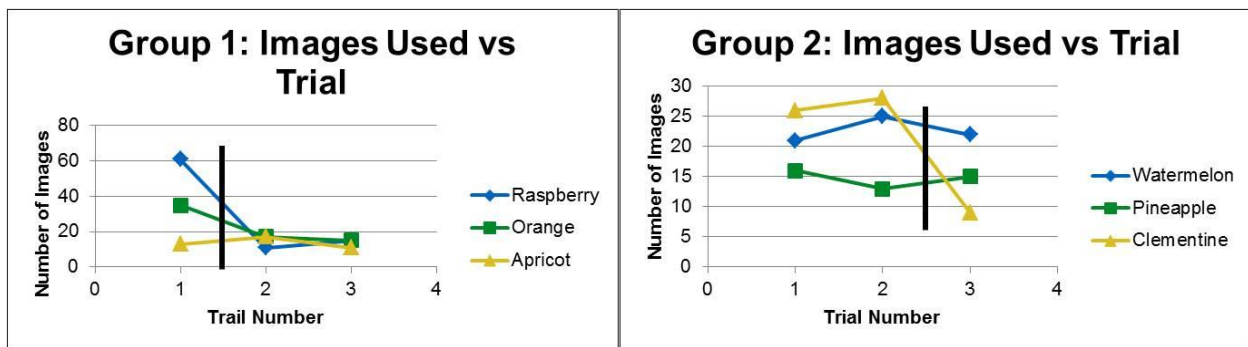


Figure 40 - The number of radiographic images used for Group 1 and Group 2 in the C-arm exercise is shown here.

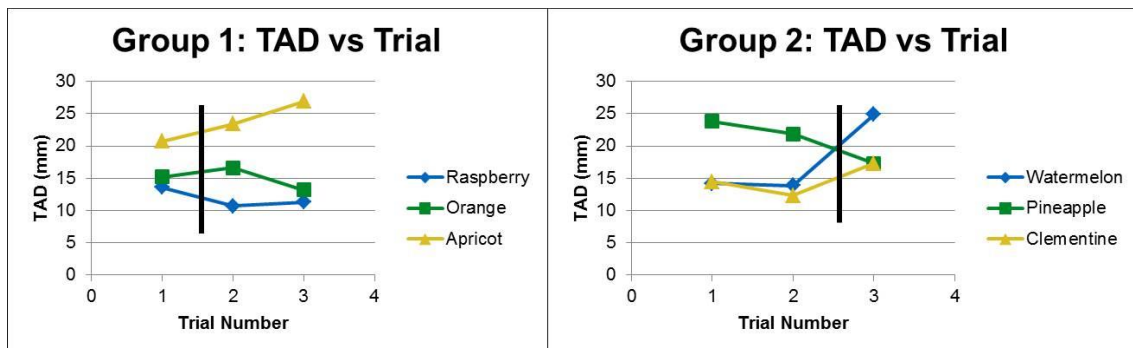


Figure 41 - The TAD results for Group 1 and Group 2 from the C-arm procedure is shown here.

To further explore the impact that training with the simulator had, the data from Group 1 and Group 2 were combined into scores achieved on the C-arm exercise before and after practicing with the simulator. Although the sample size of residents is too small to examine the significance of these results, a trend of improvement can be seen in the scores achieved after practicing with the simulator.

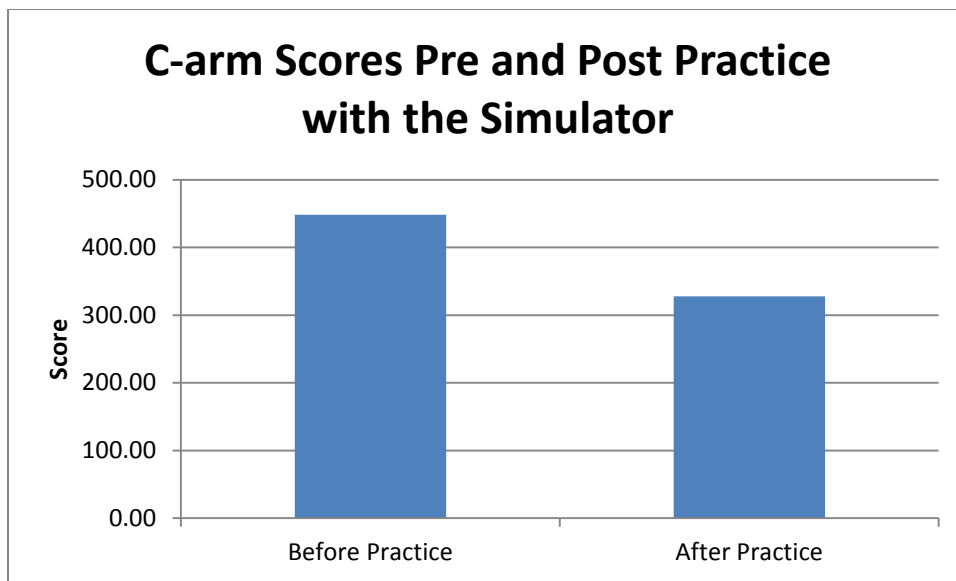


Figure 42 - Group 1 and Group 2 results are combined into pre and post practice on the simulator. A trend of improving scores can be seen in this data.

#### Discussion:

Although the number of participants that have trained on the current simulator is relatively small, we can begin to see trends in the data which point to resident behavior in learning the skill of hip wire navigation. In examining first the behavior of residents practicing on the simulator, there is a clear trend of requesting fewer fluoroscopic images and taking less time to place the guide wire as the practice session proceeded. It is interesting to note that the average tip apex distance of the residents did not experience this same trend as the residents practiced with the simulator. There could be several explanations for this observation. First, the simulator provides feedback as residents place the guide wire on what is their current tip apex distance. With this information at hand, it is likely that the guide wire was already being placed at an acceptable position and there was little room for improvement. In the first trial with the simulator, the average TAD was roughly 9mm, well below the clinically accepted threshold of

25mm. Given that the average TAD across trials on the simulator remains roughly around 10mm while the residents used less fluoro images and took less time, this points to a better understanding of the task and how to best use the fluoro images judiciously to place the guide wire accurately.

When examining the results from the C-arm exercise, similar trends can be seen. For instance, after the training session with the simulator, four out of the six residents used both fewer images to complete the procedure and took less time. Although the tip apex distance may have had a more varied trend, all six residents were able to achieve a TAD of less than 25mm on the trial immediately following training with the simulator. To put this in a different context, the residents were able to maintain clinically acceptable results while decreasing the amount of radiation exposure a patient would receive and reducing the amount of time in the OR. Reducing patient exposure to radiation has obvious health benefits and should be a goal during any surgical procedure. Additionally, time in the OR is a very expensive commodity. A study done in 2005 estimated that each additional minute in surgery can cost an average of \$62 and as much as \$133 [76]. Though the amount of time saved during this procedure may not provide overwhelming cost savings, there is the potential for this savings to be magnified when the resident surgeons enter the operating room having already had experience practicing with the wire navigation simulator.

## **Chapter 5: General Discussion and Future Work**

### Simulator Strengths and Limitations:

The main goal of this work was to develop a surgical simulator for the task of hip wire navigation. Through laboratory tests and field testing with residents, it has been shown that this goal has been achieved. The simulator developed has many strengths that make it a valuable tool to residency training programs. First, this simulator uses the same surgical tools that are used in the operating room. Given that a major goal of training on a simulator is to improve performance in the operating room, it is important that key elements of the operating room environment be preserved so that the transition between simulator and OR is relatively smooth. By using the same guide wire driver and guide wire that are used in the OR, this simulator provides a training platform that will allow for a relatively seamless transition to the operating room environment.

Providing radiation free images of the guide wire in bone is one of the greatest strengths of this simulator. As residents are just learning the task of wire navigation and are going through repeated practice sessions of the task, it is likely that they will be requesting a large number of radiographic images as they practice. Being able to provide these images with no consequence of harmful radiation allows residents the freedom to experiment with their technique, make mistakes, and keep practicing until they have perfected the task. On the other hand, if a resident were to use a C-arm to image placing a guide wire on either a radio-opaque sawbones or a cadaver bone, there would be limitations on the amount of practice that the resident could achieve. For instance, there would be a logistical limitation in the fact that fluoroscopic imaging units require a technician to operate them. Both the technician and the C-arm would come at an hourly cost and would likely not be able to stay with a resident who wanted to practice for hours on end, or more likely,

intermittently every day. Having the simulator would allow residents to practice on their own schedule and without the need for additional personnel present to operate the equipment.

In addition to providing accurate, radiation free images of the guide wire in bone, the simulator can be manufactured at a low cost, using readily available material. Most of the complexity and value in the simulator lies within the software and image processing algorithms which create the virtual radiographic images. This is advantageous to residency programs given that the results of the 2011 survey by Karam et al. suggested that most residency programs would only be willing to pay between \$1,000 and \$15,000 [45]. Compared to the cost of other wire navigation simulators currently available, this price range is relatively low. However, the simulator developed in this body of work could potentially be marketed somewhere within this price range.

The simulator also has certain limitations. One weakness of the simulator is in handling the trajectory of the guide wire when the wire is physically being bent by a resident. This causes issues because the simulator calculates the location of the wire tip inside the virtual femur based on a projection of the trajectory of wire outside of the bone. When the wire is bent outside of the bone, the trajectory is no longer in a straight line with the guide wire tip and the virtual guide wire tip is therefore calculated in a position not reflective of the true wire tip position. This can sometimes occur if a resident is trying to readjust his or her trajectory in bone and ends up bending the wire in an attempt to do so. Often times this can result in the virtual wire being displayed at a more posterior position than is true. Currently, residents are advised not to bend the guide wire to prevent this from occurring. At times residents also completely remove the guide wire driver from the guide wire so that there is no chance of bending and a true image can be obtained.

### Future Work:

Although the current results of training with residents show a trend toward improvement after training with the simulator, the sample size is too small to say whether these results are significant or not. Additional testing will be done at multiple residency programs around the Midwest to fully examine how a resident's performance improves after training with the simulator. Training days are currently scheduled at the Mayo clinic and the University of Minnesota. These programs have a combined 20 first year residents who will participate in training with the simulator. Additional trips to the Chicagoland area will provide enough resident participants to clearly examine the impact of the simulator in training residents on the task of hip wire navigation.

In addition to training with other residency programs, the simulator can be expanded into other areas of surgical skill. There are a multitude of orthopaedic procedures that require using fluoroscopic imaging to place a guide wire in bone. Examining the orthopaedic surgery milestones can provide some ideas as to what other procedures would benefit from a surgical simulator to practice on. Repairing a distal radius fracture is one of the orthopaedic surgery milestones and may be a promising area to expand the simulator into. To include a more advanced skill that a year four or year five resident may be interested in practicing, the simulator could also be expanded to include placing an iliosacral screw in the treatment of a pelvic fracture. This procedure “is technically demanding because of the limitations of radiological visualization of the relevant landmarks” and “the complex anatomy...make it difficult to place the screws accurately under radiological control” [77]. Given this description by Ziran et al, it is likely that many resident surgeons would benefit greatly from a safe environment to practice this procedure in. Expanding the simulator to include these types of procedures would likely include a modification

of some of the hardware components to fit the new anatomy, as well as implementing a new bone in the virtual world of the simulator.

In addition to expanding the current simulator to other wire navigation procedures, there is a great deal of work that could be done in orthopaedics to develop a comprehensive curriculum of training platforms, similar to the work that has been done in the Fundamentals of Laparoscopic Surgery (FLS). Groups at the University of Toronto, Canada, have begun to transition to a competency based residency program instead of the more traditional temporal based programs. In the competency based programs, residents receive a great deal of structured skills training before they practice in the operating room. Several studies published by the group at the University of Toronto have examined how the residents who are participating in this competency based curriculum are comparing against residents in the more traditional program [78-80]. The goal of this new curriculum is allow residents to graduate from their program when they have been deemed competent, not simply when they have completed a five year program. If residency programs are going to switch to graduating students when they are competent, then there needs to be a platform that can accurately assess competency. Although this work has developed a platform for training residents on the task of hip wire navigation, more work would need to be done to understand what level of performance on the simulator demonstrates competency. Furthermore, additional simulation platforms will need to be developed to assess the other areas of orthopaedic surgery, such as suturing, soft tissue handling, arthroscopy, fracture fixation, and more. It is clear that there is still a great deal of work to be done in the development of different surgical simulation platforms for the field of orthopaedics.

## References

1. Bordley, J. and A.M. Harvey, *Two centuries of American medicine, 1776-1976*. 1976, Philadelphia: Saunders. xv, 844 p.
2. O'Neill, J.A., Jr., *Surgical education: foundations and values*. J Am Coll Surg, 2009. **208**(5): p. 653-62.
3. Flexner, A., Carnegie Foundation for the Advancement of Teaching., and H.S. Pritchett, *Medical education in the United States and Canada; a report to the Carnegie Foundation for the Advancement of Teaching*. Bulletin (Carnegie Foundation for the Advancement of Teaching). 1910, New York City. xvii, 346 p. incl. maps, tables.
4. Grillo, H.C., *To impart this art: the development of graduate surgical education in the United States*. Surgery, 1999. **125**(1): p. 1-14.
5. Warren, J.C., *To work in the vineyard of surgery ; the reminiscences of J. Collins Warren, 1842-1927*. 1958, Cambridge,: Harvard University Press. viii, 288 p.
6. Halsted, W.S., *The Training of the Surgeon*. Johns Hopkins Hosp Bull, 1904. **15**: p. 267-75.
7. Franzese, C.B. and S.P. Stringer, *The evolution of surgical training: perspectives on educational models from the past to the future*. Otolaryngol Clin North Am, 2007. **40**(6): p. 1227-35, vii.
8. Cameron, J.L., *William Stewart Halsted - Our surgical heritage*. Annals of Surgery, 1997. **225**(5): p. 445-458.
9. Hamdorf, J.M. and J.C. Hall, *Acquiring surgical skills*. Br J Surg, 2000. **87**(1): p. 28-37.
10. Johnson, A., *Laparoscopic Surgery*. The Lancet, 1997. **349**(9052): p. 631-635.
11. Cuschieri, A., *Whither minimal access surgery: tribulations and expectations*. Am J Surg, 1995. **169**(1): p. 9-19.
12. Bernard, H.R. and T.W. Hartman, *Complications after laparoscopic cholecystectomy*. Am J Surg, 1993. **165**(4): p. 533-535.
13. *ACGME Highlights Its Standards on Resident Duty Hours* 2001 [cited 2015 July 7th]; Available from: <http://www.acgme.org/acgmeweb/tbid/363/Publications/Papers/PositionPapers/HighlightsItsStandardsonResidentDutyHours-.aspx>.
14. *Working Conditions - Working Time Directive*. 2003 [cited 2015 July 7th]; Available from: <http://ec.europa.eu/social/main.jsp?catId=706&langId=en&intPageId=205>.
15. Kohn, L.T., et al., *To err is human building a safer health system*, in *Academic Complete*. 2000, National Academy Press,: Washington, D.C. p. xxi, 287 p.
16. Bell, R.H., Jr., et al., *Operative experience of residents in US general surgery programs: a gap between expectation and experience*. Ann Surg, 2009. **249**(5): p. 719-24.
17. Owen, H., *Early Use of Simulation in Medical Education*. Simulation in Healthcare, 2012. **7**(2): p. 102-116.

18. Maciocia, G., *History of Acupuncture*. J Chin Med, 1982. **9**: p. 9-15.
19. Schnorrenberger, C., *Anatomical Roots of Chinese Medicine and Acupuncture*. J Chin Med, 2008. **19**: p. 35-63.
20. Faria, M.A., Jr., *The death of Henry II of France*. J Neurosurg, 1992. **77**(6): p. 964-9.
21. Gelbart, N.R., *The king's midwife : a history and mystery of Madame du Coudray*. 1998, Berkeley, Calif. ; London: University of California Press. xi, 347 p.
22. *Dittrick Museum*. [cited 2016 March 2nd]; Available from: <http://dittrick.blogspot.com/2010/02/>.
23. United States. Surgeon-General's Office., et al., *The medical and surgical history of the war of the rebellion (1861-65)*. 1875, Washington,: Govt. print. off.
24. Fitts, P.M. and M.I. Posner, *Human performance*. Basic concepts in psychology series. 1967, Belmont, Calif.,: Brooks/Cole Pub. Co. x, 162 p.
25. Ericsson, K.A., R.T. Krampe, and C. Tesch-Römer, *The role of deliberate practice in the acquisition of expert performance*. 1993, Berlin-Dahlem, Germany: R. Th. Krampe. p. 363-406.
26. Ericsson, K.A., *Acquisition and maintenance of medical expertise: a perspective from the expert-performance approach with deliberate practice*. Acad Med, 2015. **90**(11): p. 1471-86.
27. Kopta, J.A., *The development of motor skills in orthopaedic education*. Clin Orthop Relat Res, 1971. **75**: p. 80-5.
28. Moulton, C.A., et al., *Teaching surgical skills: what kind of practice makes perfect?: a randomized, controlled trial*. Ann Surg, 2006. **244**(3): p. 400-9.
29. McGaghie, W.C., et al., *Does Simulation-Based Medical Education With Deliberate Practice Yield Better Results Than Traditional Clinical Education? A Meta-Analytic Comparative Review of the Evidence*. Academic Medicine, 2011. **86**(6): p. 706-711.
30. *What tools are used in laparoscopic surgery?* 2015 [cited 2016 March]; Available from: <http://www.laparoscopic.md/instruments>.
31. *Laparoscopic Cholecystectomy*. 2002 [cited 2016 March]; Available from: <http://www.surgery.usc.edu/divisions/tumor/pancreasdiseases/web%20pages/BILIARY%20SYSTEM/laparoscopic%20chole.html>.
32. *A prospective analysis of 1518 laparoscopic cholecystectomies*. The Southern Surgeons Club. N Engl J Med, 1991. **324**(16): p. 1073-8.
33. Zucker, K.A., et al., *Training for laparoscopic surgery*. World J Surg, 1993. **17**(1): p. 3-7.
34. Derossis, A.M., et al., *Development of a model for training and evaluation of laparoscopic skills*. Am J Surg, 1998. **175**(6): p. 482-7.
35. Fried, G.M., et al., *Proving the value of simulation in laparoscopic surgery*. Ann Surg, 2004. **240**(3): p. 518-25; discussion 525-8.

36. Tay, C., A. Khajuria, and C. Gupte, *Simulation training: a systematic review of simulation in arthroscopy and proposal of a new competency-based training framework*. Int J Surg, 2014. **12**(6): p. 626-33.
37. Sroka, G., et al., *Fundamentals of laparoscopic surgery simulator training to proficiency improves laparoscopic performance in the operating room-a randomized controlled trial*. Am J Surg, 2010. **199**(1): p. 115-20.
38. *Fundamentals of Laparoscopic Surgery*. . Available from: [www.flspogram.com](http://www.flspogram.com).
39. *Training Requirements*. Available from:  
[http://www.absurgery.org/default.jsp?certgsqe\\_training](http://www.absurgery.org/default.jsp?certgsqe_training).
40. Mashaud, L.B., et al., *Two-year skill retention and certification exam performance after fundamentals of laparoscopic skills training and proficiency maintenance*. Surgery, 2010. **148**(2): p. 194-201.
41. Derossis, A.M., et al., *The effect of practice on performance in a laparoscopic simulator*. Surg Endosc, 1998. **12**(9): p. 1117-20.
42. Korndorffer, J.R., Jr., et al., *Simulator training for laparoscopic suturing using performance goals translates to the operating room*. J Am Coll Surg, 2005. **201**(1): p. 23-9.
43. Calatayud, D., et al., *Warm-up in a virtual reality environment improves performance in the operating room*. Ann Surg, 2010. **251**(6): p. 1181-5.
44. Mabrey, J.D., K.D. Reinig, and W.D. Cannon, *Virtual reality in orthopaedics: is it a reality?* Clin Orthop Relat Res, 2010. **468**(10): p. 2586-91.
45. Karam, M.D., et al., *Current and future use of surgical skills training laboratories in orthopaedic resident education: a national survey*. J Bone Joint Surg Am, 2013. **95**(1): p. e4.
46. Tsai, M.D., M.S. Hsieh, and C.H. Tsai, *Bone drilling haptic interaction for orthopedic surgical simulator*. Comput Biol Med, 2007. **37**(12): p. 1709-18.
47. Swemac, *TraumaVision Interview*, S. Long, Editor. 2016.
48. Lopez, G., et al., *A cost-effective junior resident training and assessment simulator for orthopaedic surgical skills via fundamentals of orthopaedic surgery: AAOS exhibit selection*. J Bone Joint Surg Am, 2015. **97**(8): p. 659-66.
49. Blyth, P., N.S. Stott, and I.A. Anderson, *Virtual reality assessment of technical skill using the Bonedoc DHS simulator*. Injury, 2008. **39**(10): p. 1127-33.
50. Reznick, R., et al., *Testing technical skill via an innovative "bench station" examination*. Am J Surg, 1997. **173**(3): p. 226-30.
51. Anderson, D.D., et al., *Objective Structured Assessments of Technical Skills (OSATS) Does Not Assess the Quality of the Surgical Result Effectively*. Clin Orthop Relat Res, 2016. **474**(4): p. 874-81.
52. Mayne, I.P., et al., *Development and Assessment of a Distal Radial Fracture Model as a Clinical Teaching Tool*. J Bone Joint Surg Am, 2016. **98**(5): p. 410-6.

53. *Health Data Interactive*. Health Care Use and Expenditures 2012; Available from: <http://www.cdc.gov/nchs/hdi.htm>.
54. Goldacre, M.J., S.E. Roberts, and D. Yeates, *Mortality after admission to hospital with fractured neck of femur: database study*. BMJ, 2002. **325**(7369): p. 868-9.
55. Schneider, E.L. and J.M. Guralnik, *The aging of America. Impact on health care costs*. JAMA, 1990. **263**(17): p. 2335-40.
56. Little, N.J., et al., *A prospective trial comparing the Holland nail with the dynamic hip screw in the treatment of intertrochanteric fractures of the hip*. J Bone Joint Surg Br, 2008. **90**(8): p. 1073-8.
57. AAOS. *Ortho Info*. Hip Fractures 2009; Available from: <http://orthoinfo.aaos.org/topic.cfm?topic=A00392>.
58. Bolhofner, B.R., P.R. Russo, and B. Carmen, *Results of intertrochanteric femur fractures treated with a 135-degree sliding screw with a two-hole side plate*. J Orthop Trauma, 1999. **13**(1): p. 5-8.
59. Wang, J.P., et al., *Minimally invasive technique versus conventional technique of dynamic hip screws for intertrochanteric femoral fractures*. Arch Orthop Trauma Surg, 2010. **130**(5): p. 613-20.
60. Baumgaertner, M.R., et al., *The value of the tip-apex distance in predicting failure of fixation of peritrochanteric fractures of the hip*. J Bone Joint Surg Am, 1995. **77**(7): p. 1058-64.
61. Pedersen, P., et al., *Virtual-reality simulation to assess performance in hip fracture surgery*. Acta Orthop, 2014. **85**(4): p. 403-7.
62. Thomas, G.W., et al., *The Validity and Reliability of a Hybrid Reality Simulator for Wire Navigation in Orthopaedic Surgery*. IEEE Trans Human Machine Systems, 2015. **45**: p. 119-125.
63. Kho, J.Y., et al., *A Hybrid Reality Radiation-Free Simulator for Teaching Wire Navigation Skills*. J Orthop Trauma, 2015. **29**(10): p. e385-90.
64. ACGME. *Orthopaedic Surgery Requirements*. 2012; Available from: <http://www.acgme.org/acgmeweb/tabcid/140/ProgramandInstitutionalAccreditation/SurgicalSpecialties/OrthopaedicSurgery>.
65. *Digital Folien*. Available from: <http://www.digitalefolien.de/biologie/mensch/skelett/knochen4.html>.
66. Abdel, Y.I. and H.M. Karara. *Direct linear transformation from comparator coordinates into object space coordinates in close range photogrammetry*. in *Symposium on Close-Range Photogrammetry*. 1971. Falls Church, VA: American Society of Photogrammetry.
67. Hartley, R. and A. Zisserman, *Multiple view geometry in computer vision*. 2000, Cambridge, UK ; New York: Cambridge University Press. xvi, 607 p.
68. Thomson, S. *Direct Linear Transformation*. Available from: <https://me363.byu.edu/sites/me363.byu.edu/files/userfiles/5/DLTNotes.pdf>.

69. Wheeless, C.R. *Wheeless' Textbook of Orthopaedics*. 2015; Available from: <http://www.whelessonline.com/ortho/12494>.
70. FaroArm. Available from: <http://www.faro.com/products/metrology/faroarm-measuring-arm/overview>.
71. Otsu, N., *A threshold selection method from gray-level histograms*. IEEE Trans. Sys. Man. Cyber, 1979. **9**(1): p. 62-66.
72. Canny, J., *A computational approach to edge detection*. IEEE Trans Pattern Anal Mach Intell, 1986. **8**(6): p. 679-98.
73. Lewis, J.P., *Fast Normalized Cross-Correlation*. Vision Interface, 1995.
74. *3D Printers/Prototyping Equipment*. 2015; Available from: <http://www.engineering.uiowa.edu/ems/3d-printersprototyping-equipment>.
75. Zimmerman, J.B., et al., *An evaluation of the effectiveness of adaptive histogram equalization for contrast enhancement*. IEEE Trans Med Imaging, 1988. **7**(4): p. 304-12.
76. Shippert, R.D., *A study of time-dependant operating room fees and how to save \$100,000 by using time-saving products*. Am J Cosmet Surg, 2005. **22**: p. 25-34.
77. Ziran, B.H., et al., *Iliosacral screw fixation of the posterior pelvic ring using local anaesthesia and computerised tomography*. J Bone Joint Surg Br, 2003. **85**(3): p. 411-8.
78. Sonnadara, R.R., et al., *Orthopedic boot camp: examining the effectiveness of an intensive surgical skills course*. Surgery, 2011. **149**(6): p. 745-9.
79. Sonnadara, R.R., et al., *Toronto orthopaedic boot camp III: examining the efficacy of student-regulated learning during an intensive, laboratory-based surgical skills course*. Surgery, 2013. **154**(1): p. 29-33.
80. Sonnadara, R.R., et al., *Orthopaedic Boot Camp II: examining the retention rates of an intensive surgical skills course*. Surgery, 2012. **151**(6): p. 803-7.

## Appendix 1

This section provides additional information regarding the laser etch pattern on the guide wire. The pattern was designed so that each address code produces a unique peak in the normalized cross correlation during image processing. The wire is divided into small sections of length  $d$ , defined by the resolution limit of the camera. In this application  $d$  was defined as 0.5mm. Address regions are demarcated by start and stop tags which have a length of  $2d$ . Between the start and stop marks on the wire are address code positions, either etched black or left untouched, creating a binary code. The code positions are separated by untouched portions of the wire. The etch pattern begins with the shortest addresses and progresses to longer addresses. The following equation defines the etch pattern for the entire length of the wire.

$$L = \underbrace{2}_{\text{Start tag}} + \sum_{k=0}^n \underbrace{((k+1) * 2 + 1)}_{\text{address length}} * \underbrace{2^k}_{\text{permutations}} \quad (10)$$

In this equation,  $L$  is the total length of the etch pattern and  $N$  defines the number of address lengths in the overall pattern. The pattern was designed to be 200mm in length, ensuring that the addressing scheme would be visible to the cameras even if the guide wire was drilled through the femoral head. Given this parameter, there are 5 different lengths of address ( $n=5$ ). In the equation,  $k$  defines both the length of a given address and the number of permutations which exist for a given address length. For instance, if  $k$  is equal to 1, than that address will have a total length of  $7d$ , including both the start and stop nodes. In addition, when  $k$  equals 1, then there will be 2 permutations of addresses with a length of 7. Figure 43 provides several examples of addresses with a given length and  $k$  value.

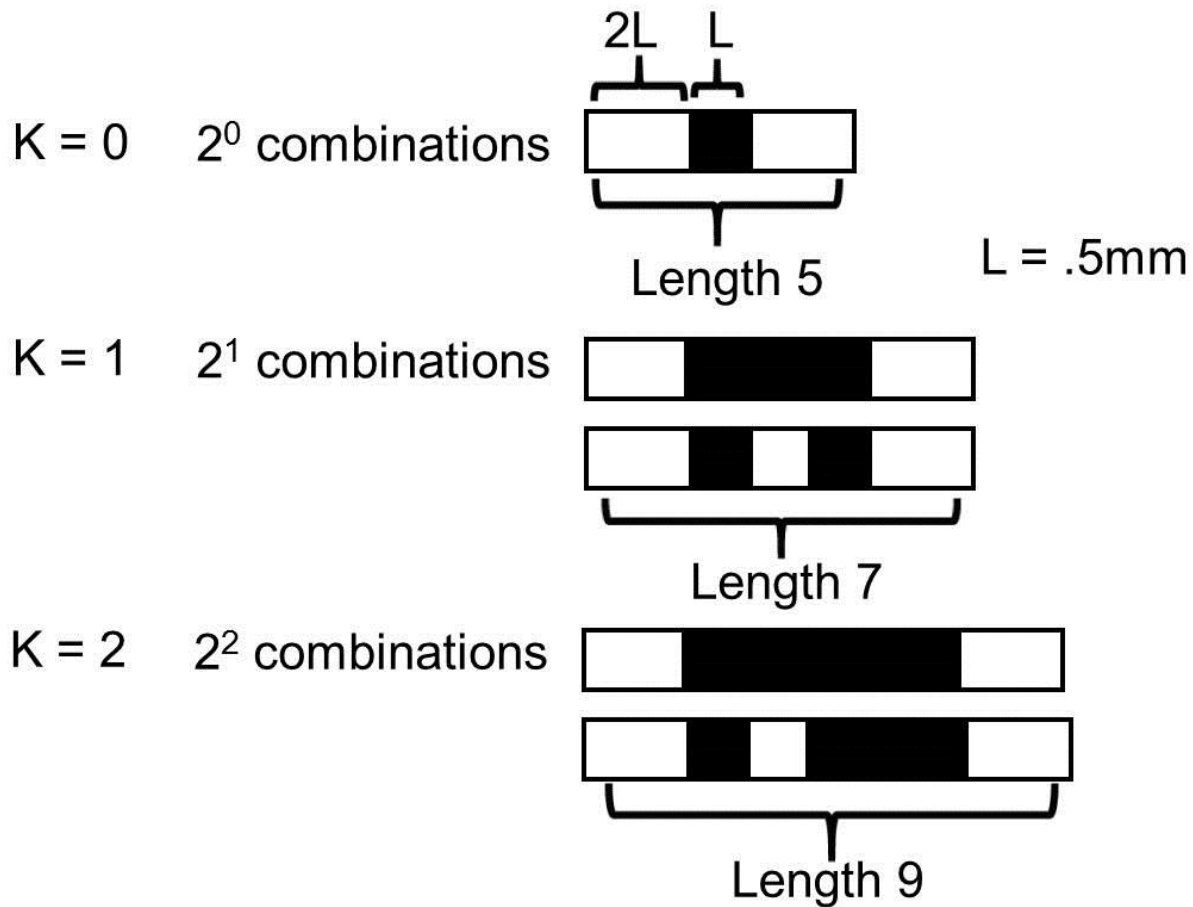


Figure 43 - Examples of different address markings are shown here. Not all combinations for  $k=2$  are shown here.

As the value of  $k$  increases, the wire addresses become longer and have increasing combinations of how the binary units can be turned “on” or “off”. The overall etch pattern can be seen below in Figure 44.



Figure 44 - The overall etch pattern on the wire is shown here. The pattern begins on the left and moves to the right.